Chemical Substances and Biological Agents

Studies and Research Projects

REPORT **R-754**

Development of a Procedure to Measure the Effectiveness of N95 Respirator Filters against Nanoparticles

Fariborz Haghighat
Ali Bahloul
Jaime Lara
Reza Mostofi
Alireza Mahdavi

irsst
nano québec

Established in Québec since 1980, the Institut de recherche Robert-Sauvé en santé et en sécurité du travail (IRSST) is a scientific research organization known for the quality of its work and the expertise of its personnel.

OUR RESEARCH is *working* for you !

Mission

To contribute, through research, to the prevention of industrial accidents and occupational diseases as well as to the rehabilitation of affected workers.

To offer the laboratory services and expertise necessary for the activities of the public occupational health and safety prevention network.

To disseminate knowledge, and to act as scientific benchmark and expert.

Funded by the Commission de la santé et de la sécurité du travail, the IRSST has a board of directors made up of an equal number of employer and worker representatives.

To find out more

Visit our Web site for complete up-to-date information about the IRSST. All our publications can be downloaded at no charge.
www.irsst.qc.ca

To obtain the latest information on the research carried out or funded by the IRSST, subscribe to Prévention au travail, the free magazine published jointly by the IRSST and the CSST.
Subscription: 1-877-221-7046

Legal Deposit
Bibliothèque et Archives nationales du Québec
2012
ISBN: 978-2-89631-639-7 (PDF)
ISSN: 0820-8395

IRSST – Communications and Knowledge Transfer Division
505 De Maisonneuve Blvd. West
Montréal, Québec
H3A 3C2
Phone: 514 288-1551
Fax: 514 288-7636
publications@irsst.qc.ca
www.irsst.qc.ca

Chemical Substances and Biological Agents

Studies and Research Projects

REPORT **R-754**

Development of a Procedure to Measure the Effectiveness of N95 Respirator Filters against Nanoparticles

Fariborz Haghighat[1], Ali Bahloul[2], Jaime Lara[3], Reza Mostofi[1], Alireza Mahdavi[1]

[1]Civil and Environmental Engineering, Concordia University
[2]Chemical and Biological Hazards Prevention, IRSST
[3]IRSST

Clic Research
www.irsst.qc.ca

This publication is available free of charge on the Web site.

This study was funded in the framework of an agreement between the IRSST and NanoQuébec.
The conclusions and recommendations are those of the authors.

ACKNOWLEDGEMENTS

This work was supported by the Institut de recherche Robert-Sauvé en santé et en sécurité du travail (IRSST) du Québec and NanoQuébec.

The authors would like to thank Dr. Bei Wang for her contributions to the early stages of this research work, and Ms. Christine Harries for her careful reading of the first draft.

In addition, the stimulating input and feedback of Dr. Claude Ostiguy and technical assistance of Mr. Yves Cloutier proved to be most important to the development of this research work. We would also like to acknowledge the important contributions of Bernard Caron, Pierre Drouin and Simon Demers, for their assistance and technical help to build, develop and monitor the experiments.

July 2012

ABSTRACT

There is an increasing concern about the potential health hazards posed to workers exposed to inhalation of nanoparticles (NPs). Common sources of nanoparticles in working environments include fumes and exhausts from different processes like laser ablation and milling. Nanoparticles have potential toxic properties: a high particle surface area, number concentration, and surface reactivity. Inhalation, the most common route of nanoparticle exposure, has been shown to cause adverse effects on pulmonary functions, and the deposited particles in the lung can be translocated to the blood system by passing through the pulmonary protection barriers. Filtration is the simplest and most common method of aerosol control. It is widely used in mechanical ventilation and respiratory protection. However, concerns have been raised regarding the effectiveness of filters for capturing nanoparticles.

In order to reach a certified level of health protection from exposure to NPs, filtering face-piece respirators are widely used by workers. N, R and P Series are three classes of such respirators approved and certified by the National Institute of Occupational Safety and Health (NIOSH). The N95 face-piece respirator is one of the most commonly used masks. Serving a broad range of industries, N95 face piece respirators are known for their disposability, low cost, suitability, etc. According to NIOSH standards (42 CFR 84, NIOSH, 1997), N95 respirators are approved to remove at least 95% of 300 nm particles under an airflow rate of 85 liters/min. NIOSH uses the average particle size of 300 nm for the approval tests, because they correspond to the most penetrating particle size (MPPS) on mechanical filters. However, previous studies demonstrated that the MPPS shifts to smaller particle sizes for electrostatic charged filters. However, a lot of information is lacking to characterize the performance of respiratory filters for nanoparticles in the different situations encountered in the working environment. Examples include the effect of temperature, humidity and respiratory flow rates.

In this study, the performance of one model of N95 NIOSH approved filtering face-piece respirator (FFR) was characterized against poly-dispersed and mono-dispersed NPs using two different experimental set-ups. With poly-dispersed NPs, a methodology was developed to measure the performance of the N95 respirators against NaCl aerosols in the size range of 15 to 200 nm in three scenarios. First, the initial particle penetration through N95 respirator was examined at four constant airflow rates: 85, 135, 270 and 360 liters/min. Second, the effect of time on the particle loading was investigated for duration of five hours. Third, the effect of the relative humidity (RH) (10, 30 and 70%) on the particle penetration was assessed at 85 liters/min.

In addition, the FFR performance was also characterized at 85 liters/min against twelve mono-sized NaCl aerosols with sizes ranging from 20 to 200 nm. The results were compared with the initial penetrations of the corresponding particle size on the FFR tested against poly-dispersed aerosols.

Using the poly-dispersed aerosols test (PAT) method, the results demonstrated that the initial particle penetration was significantly enhanced with the increased airflows and a shift toward smaller particle size was observed for the most penetrating particle. The particle penetration decreased with further loading, while a gradual increase in penetration was observed for the larger particle sizes. The MPPS was also found to shift toward the larger sized particles; from 41 to 66 nm. In addition, for the particles below 100 nm, the particle penetration augmented slightly as the RH increased. However, for the larger size particles, penetration was similar at RH of 10 and 30%; and subsequently increased as RH elevated to 70%.

The mono-dispersed aerosol test (MAT) method was performed at 85 liters/min constant flow rate; the initial particle penetration at the MPPS was below 5% NIOSH certification criterion. Moreover, the initial particle penetration value, measured with MAT method was higher than the one measured with PAT method at each corresponding particle size.

TABLE OF CONTENTS

LIST OF FIGURES

LIST OF TABLES

LIST OF ABBREVIATIONS

Abbreviation	Description
ASHRAE	American Society of Heating, Refrigerating, and Air-Conditioning Engineers
CFR	Code of Federal Regulations
CMD	Count Median Diameter
CPC	Condensation Particle Counter
CV	Coefficient of Variation
DHHS	Department of Health and Human Services
DMA	Differential Mobility Analyzer
DOP	Dioctyl Phthalate
DOS	Dioctyl Sebacate
FFR	Filtering Face-piece Respirator
GSD	Geometric Standard Deviation
HEPA	High-Efficiency Particulate Air
Kr	Krypton
MAT	Mono-dispersed Aerosol Test
MPPS	Most Penetrating Particle Size
NaCl	Sodium Chloride
NIOSH	National Institute for Occupational Safety and Health
NP	Nanoparticle
PAT	Poly-dispersed Aerosol Test
RH	Relative Humidity

SCENIHR	Scientific Committee on Emerging and Newly Identified Health Risks
SMPS	Scanning Mobility Particle Sizer
UFP	Ultrafine Particle

LIST OF SYMBOLS

English Symbols	Description
C_{down}	Downstream Concentration
C_{up}	Upstream Concentration
Dp	Particle Size Diameter
K_B	Boltzmann Constant
M	Molecular Weight
P	Particle Penetration
Q	Airflow Rate
q_f	Quality Factor
R	Correlation Ratio
T	Absolute Temperature
Z	Electrical Mobility

Greek Symbols	Description
η	Total Collection Efficiency
Δp	Pressure Drop

CHAPTER 1

BACKGROUND

1.1. Introduction

The term nanoparticles (NPs) basically refer to that range of particles below 100 nm in size, at least in one axis. NPs can be introduced in the environment from different sources; they can be associated with either natural phenomena, human or domestic activities (Crooks, 2007). There is also a new source of nanoparticle emission to the environment known as the engineered NPs, which comprises laser ablation, milling, grinding and polishing (Rengasamy, 2008a). However, it is not clear yet to what level these new sources of engineered NPs contribute to the total emissions.

In spite of very low mass concentration, the number of NPs in the environment can be very high. Thus, human exposure to NPs could be significantly more dangerous to human health than exposure to larger particles. The Scientific Committee on Emerging and Newly Identified Health Risk (SCENIHR, 2006) indicated that there could be roughly 10,000 to 20,000 NPs in the air of a normal room and 50,000 and 100,000 NPs per cubic cm in wooded and urban areas, respectively. Oberdorster (2005) has also reported the relationship between the particle number concentration, the surface area of particles and the particles diameter with the same airborne mass concentration of 10 $\mu g/cm^3$ (Table 1-1). As noticed in this table, with the same mass concentration, as the particle size diameter reduces, the number of particles drastically increases along with the exponential growth in particle surface area.

Table1-1: Number concentration and surface area of particle vs. particle diameter (Adapted from Oberdorster, 2005)

Airborne mass concentration ($\mu g/cm^3$)	Particle size (nm)	Particle number concentration (particles/cm^3)	Particle surface area ($\mu m^2/cm^3$)
10	5	153,000,000	12,000
10	20	2,400,000	3,016
10	250	1,200	240
10	5,000	0,15	12

Over the past decade, remarkable research has been done to improve the quality and functionalities of products by modifying the characteristics of their material structure at the nano-level. This technology, termed nano-technology, has been applied to the manufacturing of a wide variety of products.

It is believed that workers could be more exposed to NPs during the manufacturing of different products and this could have potential impact on workers health. According to the Bureau of Labor Statistics and the National Institute for Occupational Safety and Health (NIOSH), in 2000, in the U.S., approximately 2 million people worked with nano-material products (NIOSH, 2003). Epidemiological assessments have clearly shown acute and chronic effects related to the exposure to ultrafine particles (UFPs). Acute toxicity studies on the effects of NPs on animals have also shown acute effects on different organs; however, chronic studies are still very limited and more investigation is vital (Ostiguy et al. 2008).

Findings from the previously mentioned limited toxicological studies demonstrated that for the same mass, under similar conditions, a specific chemical is normally more toxic at the nano-metric size range than that at the micrometric size range (Donaldson et al. 2001; Oberdorster, 2000). The toxicity of the NPs was found to escalate remarkably with the increase of the particles' surface area and number concentration (Tran et al. 2000). This high surface area results in the higher surface reactivity of NPs which influences their potential toxicity in the presence of more molecules on the surface (Tran et al. 2000; Warheit et al. 2007a; Warheit at al. 2007b).

In general, workers are exposed to NPs through a wide variety of routes in work environments. These include inhalation, skin absorption, eye contact and ingestion. Inhalation is considered the most common route through which NPs reach the various parts of the living organism. When compared with larger particles, a greater portion of inhaled NPs can penetrate into the lungs where they are deposited and then translocated to other parts of the body and deposited on organs such as the brain and the heart, and in the blood system (Nemmar et al. 2001; Oberdorster et al. 2002; Ostiguy et al. 2008). A portion of these inhaled NPs are translocated to the brain via olfactory and trigeminus nerve, as observed on rats and mice (Oberdorster et al. 2004; Oberdorster et al. 2005). Moreover, they can be transported to the blood system by passing through the pulmonary protection barriers (Takenaka et al. 2001; Nemmar et al. 2002; Oberdorster et al. 2002). In this regard, the toxicity studies in rats and mice have shown that the exposure to NPs causes pulmonary diseases, cardiovascular problems and immune system impairments (Huang et al. 2007; Dockery et al. 1994; Hagdnagy et al. 1998).

Wide ranges of engineering control systems have been proposed to reduce or eliminate the exposure to NPs. These systems include enclosures, local exhaust systems, fume hoods, and general ventilation systems. If engineering controls are insufficient to ensure workers' safety and health, respiratory protection and personal protective equipment using filtration could be used to trap the NPs. The question now is "how effective are these filters to protect workers against NPs?" The effectiveness of respiratory filters is generally characterized by an airflow rate of 85 liters/min or less. However, few studies have been done on the effectiveness of respiratory protections against NPs at high airflow rates (in the case of respiratory peaks with airflow rates ranging from 300 to 400 liters/min at heavy workloads). The result of earlier (limited) work showed that high airflow rates lead to an increase in particle penetration through respirators (Richardson 2006). The effect of other parameters, such as particle size, humidity and time of use on the performance of the respirator filters remains also unknown. Therefore, with the

growth in the manufacturing sector of nano-products, it is essential to develop a method for measuring the effectiveness of respiratory protections and comparing their performances. To our knowledge, there exists no current standard to quantify or classify the performance of these filters against NPs.

1.2 Previous works

There are various key factors which affect the efficiency of the fiber filters in capturing particles such as particle characteristics (physical state, chemical composition, diameter, density and charge distribution), filter characteristics (substrate, fiber diameter, thickness of the filter, packing density of fiber and electrical property), collection mechanisms, operational conditions (temperature, viscosity and filtration face velocity) (Davies, 1973; Dullien, 1989) and thermal rebound due to Brownian motion.

Particle removal is mainly performed by two major mechanisms; mechanical and electrostatic mechanisms. The mechanical mechanism is associated with inertial impaction, gravitational interception and diffusion caused by Brownian motion. However, compared with the other mechanical mechanisms, the inertial impaction and gravitational mechanisms are normally ignored and not significantly considered in calculations for capturing small particles; these two mechanisms are more dominant to capture the large size particles (basically above 500 nm). Meanwhile, the effect of Brownian motion becomes more important for particle collection with diameter smaller than 100 nm, particularly below 10 nm (Brown, 1993; Hinds, 1999). On the other side, the electrostatic attraction force is the other collection mechanism, mainly due to Coulombic and dielectrophoretic forces between filter fibers and particles (Davies, 1973). The parameters which can affect the filtration performance with the help of the electrostatic attraction are the amount of charge on the particles, the surface charge density of fibers and the electric field applied externally (Wang, 2001).

Recent investigations show that, with the aid of both mechanical and electrostatic mechanisms, the filtration efficiency would significantly improve in particle collection (Balazy et al. 2006a; Huang et al. 2007; Eninger et al. 2008). Electret filters (using electrostatic forces) were firstly developed by Nicolaig Louis Hansen for particle removal (Davies, 1973). Hansen found the electret filters to be more effective than the mechanical filters in capturing particles. Rather than increasing the filtration performance, the electret filter media offers lower airflow resistance than the mechanical filters, due to its low packing density. A comprehensive review of the literature on the filtration performance of mechanical filters and respirators against nanoparticles has been carried by Mostofi et al. (2010).

1.3. Filtration mechanisms and models

1.3.1 Particle filtration mechanisms

As discussed earlier, particle removal is performed by four main collection mechanisms: (1) inertial impaction, (2) interception, (3) diffusion and (4) electrostatic attraction, as illustrated in Figure 1-1 (Hinds, 1999). The first three collection mechanisms refer generally to mechanical filters and are influenced by particle size.

- Inertial impaction occurs when the particle near a filter fiber changes its streamline direction and collides with the fiber (DHHS, 2003). This collection mechanism becomes more important for capturing large particles and increases at higher face velocities.
- Interception occurs when a particle follows a certain gas streamline and comes within one particle radius of a filter fiber (DHHS, 2003). Soon after, the particle touches the fiber; it will be removed from the gas flow.
- Diffusion occurs when the random motion of the particle, due to Brownian motion, causes the particle to touch the filter fiber (DHHS, 2003). The diffusion is dependent on face velocity and particle size as well. At lower face velocities, the diffusion becomes more dominant because the particle has more time for zigzag motion, thus a greater chance to collide and be captured by the filter fibers. Moreover, the small size particles have more chance to be captured by this mechanism as they behave like gas molecules with more random motion.
- The electrostatic mechanism which plays a significant role in electret filters is due to electrostatic attraction between particles and filter fibers, mainly as a result of Coulombic and dielectrophoretic attraction forces.

However, for nano-sized particles, the inertial impaction mechanism does not significantly contribute to capturing mechanisms and is thus not considered in calculations as it is more predominant for the collection of larger size particles. Also note that the effect of Brownian motion is more significant as the particles become smaller, particularly for the particles within the nano-size ranges (Brown, 1993; Hinds, 1999).

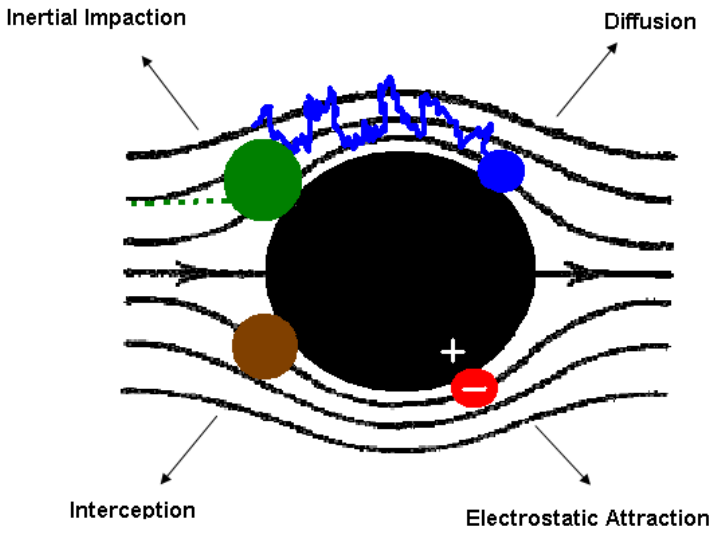

Figure 1-1: Four primary particle collection mechanisms (from Hinds, 1999).

Figure 1-2 illustrates the combined effect of the first three mechanisms (inertial impaction, interception and diffusion) on the penetration as a function of the particle diameter. In general, diffusion is considered as the predominant collection mechanism for nanometric particles, while the interception and inertial impaction are dominant for the micrometric particles. This figure demonstrates that for particles below 100 nm, with the absence of electrostatic attraction between filter fibers and particles, penetration will be reduced as the particles become smaller. This is mainly due to the fact that the diffusion mechanism is predominant in this size range. For particles with a diameter between 100 to 400 nm, both diffusion and interception contribute to the removal of particles by filters. However, in this latter size range, particles are not captured as effectively as they are at smaller diameters by diffusion, nor as effectively as they are at larger diameters by interception and impaction. Therefore, this size range is generally considered the worst-case situation and it experiences the greatest penetration through the filter. Finally, for particles larger than 400 nm, penetration will decrease again as both the interception and inertial impaction effects significantly contribute to the collection of particles (Lee et al. 1980).

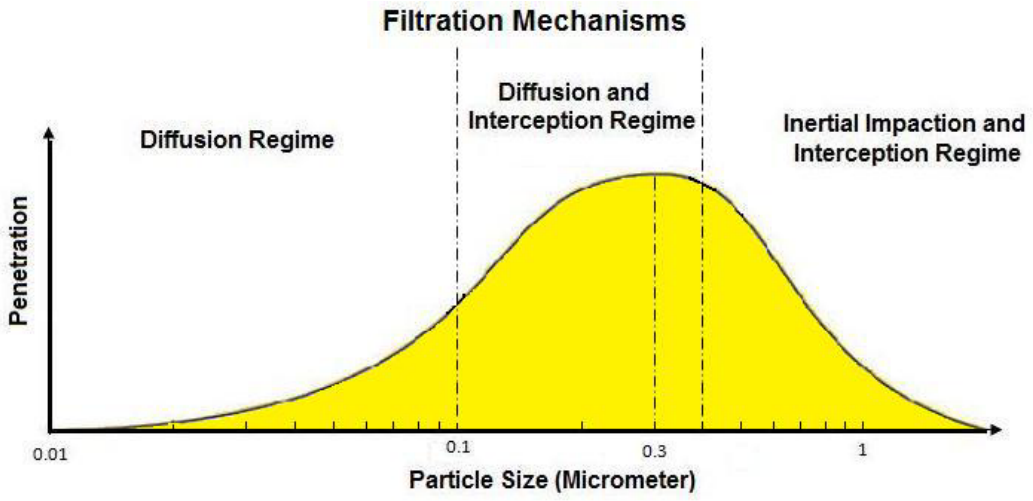

Figure 1-2: Fractional penetrations vs. particle diameter for a mechanical filter.

However, it should be mentioned that in the classic collection efficiency curve, for the electret respirator filters, the minimum filtration efficiency for the most penetrating particle size (MPPS) can be shifted toward small particle sizes, lower than 100 nm (Han, 2000; Martin and Moyer, 2000; Huang et al. 2007; Rengasamy et al. 2007; Eninger et al. 2008).

1.3.2. Most penetrating particle size (MPPS)

Previous studies have indicated that the mechanical and electret filters have different performance in aerosol collection within the nano-sized range. In general, for mechanical (non-charged) filters, a particle diameter of 300 nm is referenced as the MPPS at 85 liters/min, while for electret filters (charged), the lowest filtration efficiency could occur for a particle much smaller than 300 nm in size. In this regard, particle penetration through both mechanical and electret filters were investigated for particles between 4.5 nm to 10 µm by Huang et al. (2007). They reported that the maximum penetration was reduced from 18.9 to 5.8% with the co-operation of an electrostatic attraction force in particle collection. They demonstrated that the MPPS shifted toward the smaller particle using electret filters. The MPPS occurred at 50 nm for electrets and 200 nm when the charge was removed from the filter fibers.

Kanaoka et al. (1987) reported that the maximum penetration through electrostatically-enhanced filters occurred for uncharged particles from 30 to 40 nm in size, whereas singly charged particles showed a peak at a much larger size. Balazy et al. (2006a) measured the penetration of the MS2 viruses (a non-harmful stimulant of several pathogens) through face-piece respirators. The study was carried out for particles ranging from 10 to 80 nm, at airflow rates of 30 and 85 liters/min. The MPPS was observed around 50 nm for tested respirators. The results also showed that the penetration through the electrets N95 respirators could exceed up to 5.6% in the MPPS at 85 liters/min. However, N95 respirators are expected to provide 95% filtration efficiency against non-biologic and biologic particles in the MPPS. Balazy et al. (2006b) measured the filtration

performance of N95 respirators for NaCl particles in the size of 10 to 600 nm based on a manikin-based protocol. The respirators were tested at airflow rates of 30 and 85 liters/min, and the observed MPPS for the respirators with pre-charged filter media was between 30 to 70 nm. Martin and Moyer (2000) also investigated the most penetrating particle size for electret filters, and found that the MPPS was in the size range from 50 to 100 nm for electret filters and it shifted to larger sizes from 250 to 350 nm if the filters were dipped in isopropanol (to reduce the electrical charge on the filter fibers). Richardson et al. (2006) tested N95 face-piece respirators with electret filter media using neutralized NaCl, dioctyl phthalate (DOP) and MS2 aerosols, and the observed MPPS was smaller than 100 nm. Eninger et al. (2008) also found that for electrets filters, the MPPS appears to be less than 100 nm for uncharged and Boltzmann charged aerosols. Rengasamy et al. (2007) investigated the penetration of N95 respirators using Boltzmann-charged NaCl aerosol in the size range of 20 to 400 nm. They reported a MPPS of around 40 nm.

These studies showed that the MPPS strongly depends on factors such as filter properties, filtration mechanism, airflow rate, fiber charge density and aerosol particle charge distribution. For non-charged fibers, the MPPS was generally within the size range of 100 to 400 nm, and the MPPS would increase with increasing fiber diameter and decreasing airflow rate (Grafe et al. 2001; Howard, 2003). For charged filter media, the MPPS significantly depended on the fiber charge conditions (Martin and Moyer, 2000).

1.4. Filtration efficiency affecting factors

1.4.1. Face velocity and airflow rate

The face velocity/airflow rate can significantly affect the total filtration performance of fibrous filters since it influences the contribution of diffusion, interception and electrostatic mechanisms (Kousaka et al. 1990; Alonso et al. 1997). At low face velocity, diffusion and electrostatic forces significantly contribute to the capture efficiency due to higher residence time. With an increasing face velocity, the interception mechanism dominates while the diffusion effect contributes much less to the filter collection performance. Thus, it is expected that the filtration efficiency drops considerably at higher face velocity. Boskovic et al. (2007, 2008) tested the filtration efficiency at various velocities ranging from 5 to 20 cm/s for different shapes of particles (sphere, semi rounded and cubic). The measured particle size was in the range of 50–300 nm. The results showed that at lower face velocity the filtration efficiency of fibrous filters improved for all different shape of particles. Balazy et al. (2004) investigated the filtration efficiency and pressure drop at air velocities between 10 and 30 cm/s for particles in the range of 10–500 nm. The results demonstrated that the total filtration efficiency was reduced by increasing air velocity. Kim et al. (2007) conducted the penetration test at face velocity of 5.3, 10, and 15 cm/s using silver nanoparticles from 3 nm to 20 nm. The results showed that higher face velocity increases particle penetration due to shorter residence time through filters.

For respiratory filters, particle penetration is determined as a function of the airflow rate instead of face velocity. Several studies have been conducted to investigate the effectiveness of

respirators in the removal of nanoparticles at different airflow rates. Eninger et al. (2008) evaluated the performance of two models of N95 and one N99 face-piece respirators against three viruses and NaCl particles. Experiments were carried out at airflow rates of 30, 85 and 150 liters/min. For the N95 model, the highest NaCl particle penetrations of 1.3, 5.9 and 10.2% were obtained at respectively airflow rates of 30, 85 and 150 liters/min. For the N99 respirator model, the maximum penetrations were 1.0, 4.3 and 6.6% at airflow rates of 30, 85 and 150 liters/min, respectively. For the viruses, an increase of airflow rate from 85 to 150 liters/min strongly affected the performance of all tested respirators. Balazy et al. (2006b) also measured the penetration through two models of N95 respirators for NaCl particles within 10 to 600 nm at two airflow rates of 30 and 85 liters/min. The results demonstrated that airflow rate has a strong impact on the particle penetration through the filter face-piece respirators. Particle penetration through both N95 respirators would exceed up to 5% at the airflow rate of 85 liters/min. Rengasamy et al. (2008a) evaluated the performance of several N95 and P100 models against mono-dispersed silver aerosols. The test was carried out for particles ranging from 4 to 30 nm at an airflow rate of 85 liters/min. The results demonstrated that the particle penetration decreased for all tested respirators as the particle size decreased to 4 nm. For N95 face-piece respirators, the particle penetration varied from 1.1 to 4.0%. For P100 respirators, a particle penetration less than 0.3% was observed.

Most existing guidelines suggest testing filters at the flow rate of 85 liters/min as this flow rate simulates human breathing at a heavy work load. Janssen (2003) however suggested that respirators should be tested at an airflow rate of 350 liters/min; it is believed that a much higher breathing airflow rate may occur in the workplace.

1.4.2. Humidity

Humidity is one of the factors that may influence the filtration performance. The effects of humidity are not well understood due to a lack of investigations. Kim et al. (2006) reported no significant effect of humidity on filtration efficiency for particles below 100 nm by showing almost the same filtration efficiency at relative humidity (RH) of 0.04, 1.22, and 92%. Inconsistent with Kim et al.'s observation, Brown (1993) and Miguel (2003) showed that the filtration efficiency improved with increasing relative humidity for coarse particles. Kim et al. (2006) explained that an increase of the capillary force at higher RH would increase the adherence between filter fibers and particles. However, the high attraction between particles and filters due to capillary force is only considerable for larger size particles.

In contrast to studies for mechanical filters, the studies for electret filters (charged filters) demonstrated that the filtration performance decreases as the humidity increases. The reason is that higher humidity would lead to a reduction in the charges on the filter fibers and on the particles (Ackley, 1982; Moyer et al. 1989). Ikezaki et al. (1995) and Lowkis et al. (2001) also confirmed that the potential of the electret filters on the collection of particles fell as the surface charge decreased with an increase in RH. Yang and Lee (2005), however, reported that RH had no effect on the aerosol penetration through electret filters for mono-dispersed NaCl particles

ranging from 50 to 100 nm by showing that the aerosol penetration was almost the same at two RH of 30 and 70%. Yang and Lee (2005) explained that other studies mainly charged the electret filters either by using corona or triboelectric charging methods. These methods made the ions and electrons on the fibers easily removable by the water molecules (resulting in the decrease of surface charge with a higher RH). In their study, Yang and Lee (2005) charged filters by coating with negative carbon-chain-group ions which makes the surface charge less affected by the humidity. Another possibility is that NaCl particles at RH of 70% may undergo deliquescence and grow into larger particles so that the measured filtration efficiency is overestimated.

1.4.3. Particle loading

Particle loading is one of the other important aspects which influence the filtration performance. The feedback effect of particle loading is less well understood. According to the literature, the subsequent particle loading implies a significant impact on the collection efficiency and also on the pressure drop evolution across a filter (Baumgartner et al. 1986; Brown et al. 1988; Chen et al. 1993; Martin and Moyer, 2000; Wang et al. 2001). With the absence of an electrostatic effect, the continuous particle loading generally results in an increase in the particle collection efficiency and pressure drop, caused by the particle accumulation on the fiber surface (Wang, 2001).

In contrast with results obtained for the mechanical filters, according to the previous experimental studies on the electret filters, particle penetration generally increases during the initial stage of filter loading (Baumgartner et al. 1986; Brown et al. 1988; Chen et al. 1993; Martin and Moyer, 2000; Wang et al. 2001). However, the pattern for particle collection efficiency may change for different fiber materials and particle sizes. Chen et al. (1993) investigated the filtration performance of dust-mist filtering face-pieces loaded continuously against corn oil aerosols with size diameter of 0.16 μm. They reported that the particle penetration initially increased with aerosol loading due to a reduction in the electrostatic charge effect; however, it subsequently diminished due to the increase in packing density of the filter fibers. Brown et al. (1988) reported that the filter loading would significantly augment the penetration through the electret filters, since the electrostatic charge effect on the filter fibers is screened by the deposited aerosols. Their experiments were carried out for various industrial aerosols at different particle size ranges.

Additionally, experimental studies on electret filters showed that particle collection efficiency relies generally on the manner in which the particles are collected; exposed with solid or liquid particles (Martin and Moyer, 2000; Ji et al. 2003). Martin and Moyer (2000) used solid NaCl and liquid DOP particles to test the filtration efficiency of N95 respirators. Their results indicated more particle penetration when the N95 respirator was challenged with liquid DOP aerosols, increased by about ten folds. In another study conducted by Ji et al. (2003), the electret filters were loaded with poly-dispersed solid sodium chloride (NaCl) and liquid dioctyl sebacate (DOS) particles. Remaining consistent with the other study, much lower filtration performance occurred with testing filters against liquid DOS.

1.4.4. Particle charge state

Particle charge is another factor that significantly affects the particle filtration efficiency of mechanical and electret filters (Fjeld and Owen, 1988; Chen et al. 1998). The increase in filtration efficiency is associated with additional electrostatic attraction resulting from coulombic and image force attraction (Brown, 1993). Kim et al. (2006) demonstrated the difference in the collection efficiency through a glass fiber filter at different charge states for particle ranging from 2 to 100 nm. They found that the filtration efficiency for uncharged particles was much lower than that for charged particles, and that this discrepancy decreased with the reduction in particle size. They explained that this phenomenon was due to the fact that diffusion is the most dominant deposition mechanism for nanoparticles and this process increases the effect of diffusion for smaller particles. The penetration of neutralized and non-neutralized particle in the range of 10 to 600 nm through electret and mechanical filters was investigated by Balazy et al. (2006b). Higher filtration efficiency was observed when testing the penetration of the neutralized particles for the electret filters. However, for the mechanical filters, they reported no significant change between the neutralized and non-neutralized particles. Yang and Lee (2005) measured the filtration efficiency for NaCl aerosols with the Boltzmann-equilibrium, neutral, or singly charged state. They showed that singly charged aerosols would lead to higher filtration efficiency than neutral aerosols: the Coulombic capture force was dominant for nanoparticles.

1.5. Test standards

In June 1995, NIOSH updated the certification test criteria for negative pressure air-purifying particulate respirators with the enactment of 42 CFR 84 (CFR, 1996). NIOSH certifies three classes of filters labeled N, R, and P, and three levels of filter efficiency, 95, 99 and 99.97% for each class of filters. N, R and P correspond to filters being not resistant, with a limited resistance and resistant to oil aerosols, respectively.

N type respirators correspond to the filters with resistance against only solid aerosol (not efficient against oily aerosols), while the R and P type respirators are also intended to be fairly and highly resistant, respectively, against oily aerosols. NIOSH approves the ‘N series’ respirator filters with poly-dispersed NaCl particles with a count median diameter (CMD) of 75 ± 20 nm and a geometric standard deviation (GSD) not greater than 1.86. The R and P designated respirators are challenged against DOP with a CMD of 165 ± 20 nm and a GSD not greater than 1.60 (CFR, 1996).

The existing NIOSH certification intends to certify the N, R and P respirators at very conservative test conditions, as the performance of the filters can tremendously vary under different situations. For instance, to test filters in severe conditions, the respiratory tests at NIOSH are performed at a constant airflow rate of 85 liters/min corresponding to an average breathing rate of an individual involved under a heavy work load.

These certification tests may be used for ranking the respirators but may not always represent the worst case scenario in terms of collection efficiency (Eninger et al. 2008). For example, Balazy

et al. (2006b) showed that an emerging Coulombic force would be induced if both filters and particles were charged: this would significantly overestimate the respirator performance. As pointed out earlier, the question as to if the MPPS for a specific filter system can be shifted mainly depends on the magnitude of filtration face velocity, filter type, filtration mechanism, fiber charge density and particle charge distribution (Eninger et al. 2008). The MPPS for electret filters is much smaller than that for mechanical filters. However, the NIOSH certification test assumes a MPPS of approximately 300 nm for all filters and filter types, which may not be true for electret filters. Furthermore, forward-light scattering photometers are used in the NIOSH testing protocol to measure aerosol concentrations before and after the tested respirator.

Generally, photometer signal is only capable of measuring particles with diameters larger than 100 nm. Therefore, the photometric method deployed in the NIOSH protocol is not suitable for measuring the filtration efficiency for nanoparticles (Eninger et al. 2008). In a study carried out by Eninger et al. (2008), the results showed that 68% (by count) and 8% (by mass) of NaCl and 10% (by count) and 0.3% (by mass) of DOP particles are below 100 nm in the NIOSH testing protocol. As noted above, the photometric method used in the NIOSH protocol does not effectively contribute to measure the ultrafine particles (<100 nm). One of the other limitations in NIOSH certification is that the collection efficiency of the filter respirators is not presented in terms of the particle size; the test is only based on measuring particle mass concentration before and after filter for poly-dispersed challenged aerosols. However, as discussed previously, in spite of very low mass concentration, the number of NPs can be very high in the environment. Thus, the human exposure to NPs could be even more dangerous to human health than is exposure to larger particles.

1.6. Research objective

The objectives of this study are:

- To develop a methodology to characterize the effectiveness of one model of NIOSH-approved N95 respirator filter at constant airflow rate against poly-dispersed aerosols in size ranging from 15 to 200 nm in different scenarios:

    1. Investigating the effect of airflow condition and particle size on the initial particle penetration through the respirator and,

    2. Investigating the effect of two other parameters, such as the time of use and the relative humidity on filtration performance.

- To develop and adapt the experimental set-up to challenge the same type of respirator against mono-dispersed particles with a size ranging between 20 and 200 nm.

CHAPTER 2

EXPERIMENTAL METHOD

2.1. Introduction

A small scale test facility was used in this research and it was designed and constructed to incorporate an air-cleaning device to simulate its actual application. The duct was made of a stainless steel chamber with a Plexiglas opening in the front and back. Air supplied to the system was filtered through a High-Efficiency Particulate Air (HEPA) filter and conditioned to have a constant temperature and humidity. A HEPA filter was used to remove particles before discharging the air. The pump at the end of the unit was used for balancing the pressure inside the system, while a safety valve was controlled by a computer to balance pressure inside the chamber.

2.2. Overview of experimental set-ups

Figures 2-1 and 2-2 show the schematic diagrams of the experimental set-ups used to test respirators against mono-dispersed and poly-dispersed aerosols, respectively. These schematic diagrams also indicate the required procedures to test the respirators.

2.2.1. Filtration test against mono-dispersed aerosols

The six-Jet Collision Nebulizer (Model CN25, BGI Inc. Waltham, MA) is employed as an aerosol generator to provide particles with a size ranging from 20 to 200 nm (Figure 2-1). Next, a long differential mobility analyzer (long DMA; Model 3081, TSI Inc.) is used to extract mono-sized particles by size, classifying the charged particles based on their electrical mobility[1]. As the particles enter the DMA, they experience an external electric field causing each particle with a certain diameter to follow a specific trajectory and to migrate with a certain amount of velocity. Only specific size-selected particles within a narrow range of electrical mobility (inversely related to particle size) will have the correct trajectory to exit the DMA (Appendix B). Then, the resulting charged particles of known size exiting from the DMA are passed through the neutralizer (Kr-85) (Model 3012A, TSI Inc.) to obtain the Boltzmann charge equilibrium (Appendix C). Afterwards, according to the testing airflow rate, an extra dry-filtered airflow is added to the mono size selected aerosol flow. The total aerosol flow from the DMA and the extra introduced clean air are mixed before entering the filter test system. In addition, a small mixing fan is used at the inlet of the chamber to disperse the aerosols. A condensation particle counter (CPC) (Model 3775, TSI Inc.) is then used to monitor the particle concentration in real time at

[1] The electrical mobility is the ratio of migration velocity caused by an external force, an electric field, to the magnitude of the external force.

the downstream and at the upstream of the filter, alternately. Consequently, the filtration efficiency at the tested particle size is measured. By performing the test for different mono size particles, the particle filtration efficiency (or particle penetration) can be determined as a function of particle size.

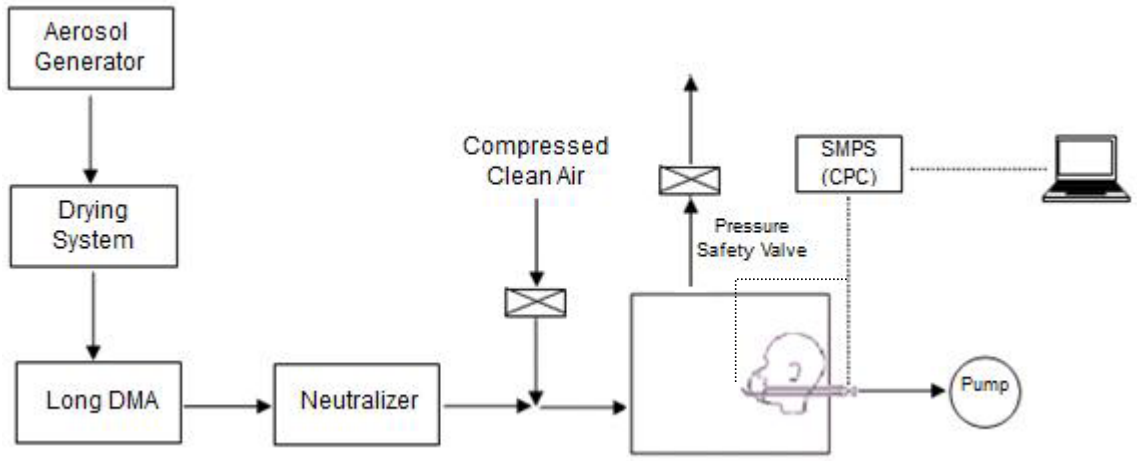

Figure 2-1: Schematic diagram of experimental set-up: testing filters against mono-dispersed aerosols under constant flow. Manikin adapted from Balazy et al. 2006a.

2.2.2. Filtration test against poly-dispersed aerosols

In this experimental set-up (Figure 2-2a), after generating poly-dispersed aerosols and passing the generated aerosols through the neutralizer, the additional required dry-clean airflow is added to the neutralized poly-dispersed aerosols (particles in the 15 to 200 nm range). Next, the mixed poly-dispersed aerosols and airflow is passed directly into the chamber. Subsequently, after allowing the system to stabilize and setting the sampling flow rate at 1.5 liters/min, the concentration and size distribution are measured alternately twice at the downstream and twice at the upstream of the test filter by a scanning mobility particle sizer (SMPS) (Model 3936, TSI Inc), which mainly consists of DMA and CPC. The required time for each measurement at either downstream or upstream is 135 seconds. This includes 30-second samplings done twice for downstream firstly and twice for upstream secondly, in addition to 15 seconds for switching samples from downstream to upstream. Consequently, the particle penetration values were determined as a function of particle diameter. The particle concentration and size distribution at airflow rates of 85, 135, 270 and 360 liters/min at upstream (used for challenging the N95 respirator against poly-dispersed aerosols) are presented in Figure 2-2b.

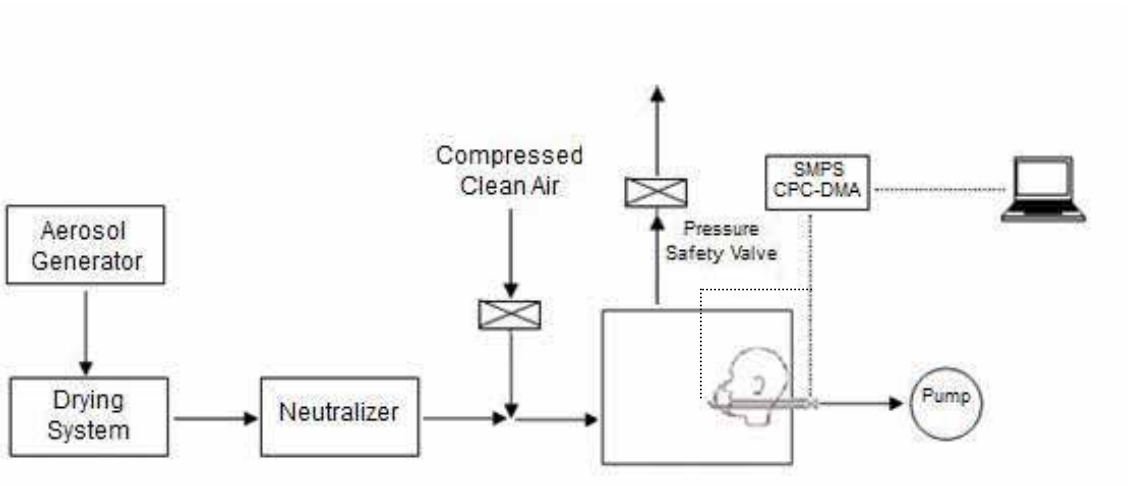

Figure 2-2a: Schematic diagram of experimental set-up: testing filters against poly-dispersed aerosols under constant flows. Manikin adapted from Balazy et al. 2006a.

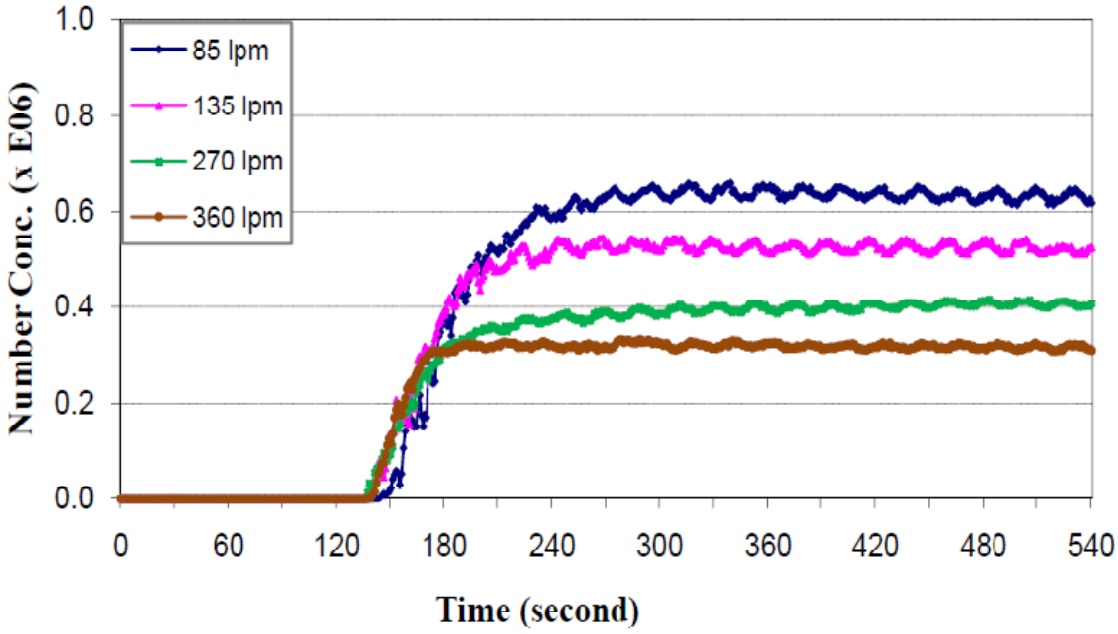

Figure 2-2b: Challenged aerosol concentration (particles/cm^3) during system start-up at different airflow rates, using 0.01% NaCl (lpm = liters/min).

2.3. Test procedure

Figure 2-3 presents the full schematic of the experimental set-up utilized to challenge tested respirators against poly-dispersed aerosols. Experiments were carried to verify the uniformity of aerosol concentration within the test chamber.

Figure 2-3: Schematic of the test system used to challenge N95 respirators against poly-dispersed aerosols.

In the case of respiratory filters, one model of NIOSH-approved N95 filtering face-piece respirators was selected to be challenged against poly-dispersed NPs (Figure 2-4). The selected N95 respirator was sealed by silicon sealant on the manikin's face and placed on the left side within the test chamber (Figure 2-5). Considering this situation, the possible leakage between the respirator and the manikin's face was not taken in the filtration efficiency analysis.

Figure 2-4: Photograph of the tested N95 respirator.

Figure 2-5: Photograph of the N95 respirator sealed on the manikin.

Images acquired by transmission electron microscopy (TEM) of poly-dispersed NaCl nano-sized particles in aerosol are showed in Figures 2-6, 2-7 and 2-8. As we can observe, the optical size of the NaCl particles seems to vary but remains in the nanometric dimension (< 100 nm), with the presence of agglomerates that can exceed the nanoscale. We also noticed that NaCl particles or agglomerates of particles had different shape and structure. Primary particles seem appreciatively spherical; however, agglomerates diverge substantially from this shape. As for the structure, as illustrated in Figures 2-7 and 2-8, NaCl particles or agglomerates could be either dense or porous, that is to say with some void space between the primary particles constituting the agglomerate. In addition, as shown in Figure 2-8, the porosity of NaCl agglomerates is not necessarily the same throughout all agglomerates that are present in the aerosol. Nonetheless, we must be cautious about the results obtained by microscopy since we have sampled nano-sized particle composed of salt, which can produce artifacts when drying into crystal or films onto the substrate, resulting in changes of shape and structure (Powers et al. 2007).

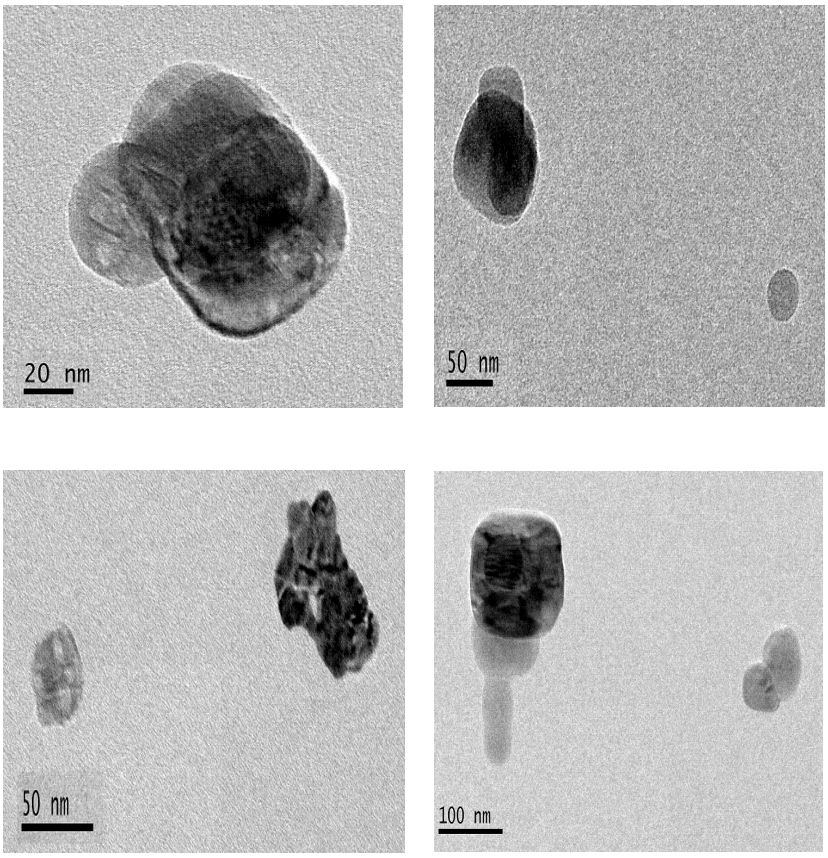

Figure 2-6: TEM images of poly-dispersed NaCl in aerosol.

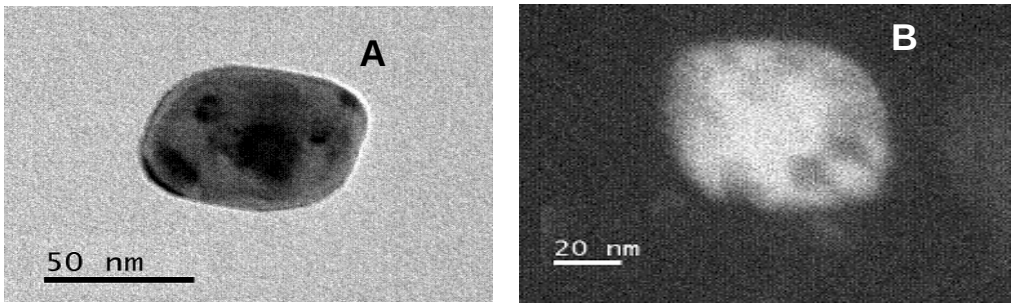

Figure 2-7: TEM images of dense (A) and porous (B) NaCl nanoparticles from aerosol.

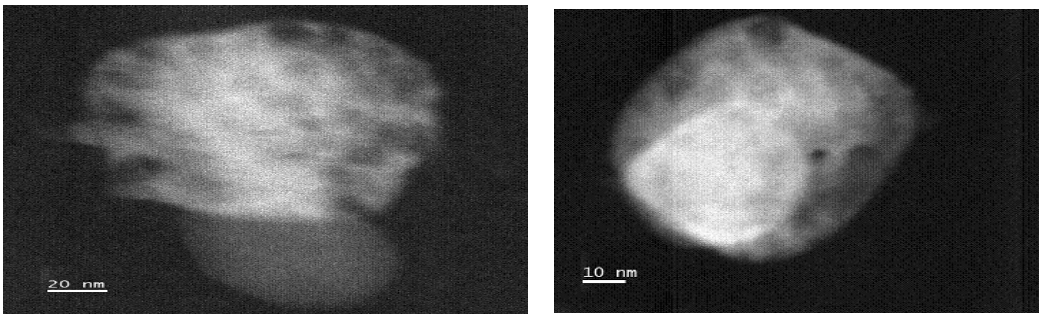

Figure 2-8: TEM images of porous NaCl nanoparticles from aerosol.

The six-Jet Collision Nebulizer was operated at an inlet pressure of 25 psi, and fed with 0.1% (V/V) NaCl solution to generate poly-dispersed NaCl particles in the 15 to 200 nm range (Figure 2-9). The challenged NaCl aerosol employed in this study, with 99.9% purity and a density of 2165 kg/m^3, was dissolved in distilled water. A filtered air supply (Model 3074, TSI Inc.) was used to provide a clean-dry air entering the generation system.

Figure 2-9: Photograph of the filtered air supply (Model 3074, TSI Inc.) connected with six-Jet Collision Nebulizer.

To remove the possible water vapor in the aerosol flow coming out from the Collision Nebulizer, a diffusion dryer was applied. The drying system was composed of an inner tube made of a wire screen and surrounded by silica gel in an outer plastic tube (Figure 2-10). In this case, as the

aerosol passed through the inner tube, the water vapor was absorbed on the porous wall and afterwards removed with the surrounding silica gel. Prior to the filtration efficiency test, in order to reach a steady state concentration at the upstream of the chamber, the generation system was allowed to operate for at least 5 minutes (for more detailed information, see Appendix A about the calibration results for the stabilization test). To reduce the chance of particle loading, the N95 respirator was bypassed during the stabilization period. Having stabilized the system, the switching valve was adjusted, letting the total aerosol flow pass directly through the test filter.

Figure 2-10: The silica gel drying system.

Subsequently, after allowing the system to stabilize and setting the sampling flow rate at 1.5 liters/min, the concentration and the size distribution were measured alternately twice at the downstream and twice at the upstream of the test filter by a SMPS. The required time for each measurement at either downstream or upstream was 135 seconds. Consequently, the particle penetration values were determined as a function of the particle diameter. The particle concentration and size distribution at airflow rates of 85, 135, 270 and 360 liters/min at upstream (used for challenging the N95 respirator against poly-dispersed aerosols) are presented in Figure 2-11.

In the experimental set-up, a pressure transducer was also applied to measure the pressure drop across the tested face-piece respirator. Thus, the quality factor $(q_f)^2$, which corresponds to the particle penetration (P, %) and airflow resistance (Δp, in mm H_2O) through the filter, was determined based on the particle size. This indicator of filter performance is defined by Brown (1993) as:

$$q_f = \frac{\ln (1/P)}{\Delta p}$$

[2] The quality factor is used as a means to categorize the filter performance in accordance with particle penetration and air resistance (Hinds, 1999).

According to the 42 CFR 84, pre-treatment at 85% relative humidity and 38°C for 25 hours is required for N series respirators. Tests carried out at the beginning of the project did not show a substantial difference in results in term of penetration of NP between the preconditioned filters and the non preconditioned ones. Therefore, the selected N95 respirators were not preconditioned for relative humidity before testing (filters were tested as received from the manufacturer). The operational conditions (temperature, pressure and relative humidity) were monitored in the chamber during the test. The temperature was maintained at the ambient temperature (23±2°C). Except for the humidity test, the relative humidity was maintained at 8 ± 2%: compressed dry air was used. A small mixing fan was housed at the inlet of the chamber.

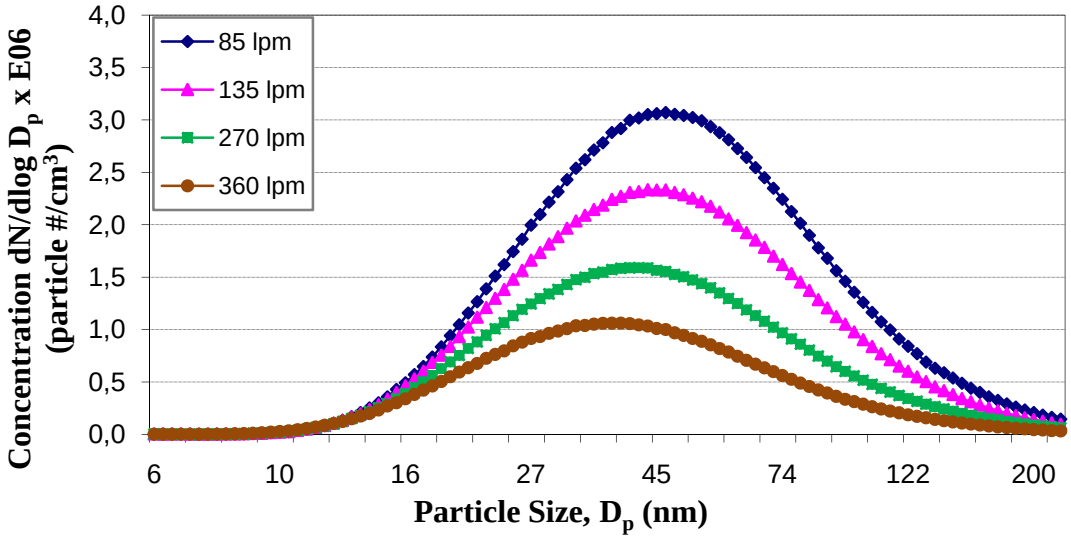

Figure 2-11: The particle concentration and size distribution of the challenged NaCl aerosol at different testing constant airflow rates (operating Nebulizer at 25 psi inlet pressure, using 0.1% NaCl solution).

In addition, to assess the effect of relative humidity on the filter performance, a Humidity Control System (MNR, Model HCS-301, Miller Nelson Research Inc.) was utilized to condition the relative humidity before the total air entered the inlet chamber.

To challenge N95 respirators against mono-dispersed aerosols, the same testing procedure as discussed above was followed, except that the experimental set-up was adapted to be capable of testing filters with mono-dispersed particles (see Figure 2-1 on p. 14).

After generating poly-dispersed aerosols using the six-Jet Collision Nebulizer (operated at an inlet pressure of 25 psi, using 0.1% NaCl solution) and passing the generated aerosols through

the silica gel drying system and neutralizer (Kr-85), a long DMA was utilized to extract mono-sized particles before entering the filter test system.

A CPC was used to count the particle concentration of each selected mono-sized particle at both the downstream and the upstream of the filter. The challenged mono-sized NaCl aerosols were pumped for 2 minutes with CPC at a sampling flow rate of 1.5 liters/min both at the downstream and the upstream. To provide a reliable sampling condition, the particle counter instrument was allowed to stabilize after switching between the two sampling ports at the downstream and upstream. Consequently, the percentage penetration was measured for each tested mono-sized particle.

2.4. Filtration efficiency measurement

The particle penetration through the filter is determined as the ratio of the downstream concentration (C_{down}) to the upstream concentration (C_{up}) for each challenged particle size, and is presented as follows:

$$P(\%) = \left(\frac{C_{down}}{C_{up}}\right) * 100$$

Consequently, the total collection efficiency (η), as a function of particle size is defined as:

$$\eta(\%) = (\frac{C_{up} - C_{down}}{C_{up}}) * 100 = 100 - P$$

The concentration (of whether upstream or downstream) applied in the above formulas is the number concentration which is defined as the total number counted by SMPS along with the CPC. Note that according to the measurement technique, the total collection efficiency can be determined in terms of mass or number concentration.

In this project, the performance of the N95 filter was verified with the poly-dispersed aerosols test (PAT) and the mono-dispersed aerosols test (MAT), under different conditions such as varying airflow rate, relative humidity (RH) and loading times. Each respirator was tested three times for initial penetration. Table 2-1 summarizes the experimental measurements performed in the current study.

Table 2-1: Summary of experimental measurements

Poly-dispersed aerosol test (PAT) ***(Particle size from 15 to 200 nm)***		
Varying Parameter	**Values**	**Fixed parameters**
Airflow rate	85, 135, 270 and 360 liters/min (n=3)	Loading time = 0 RH = 8 ± 2%
Loading time	0, 1, 2, 3, 4 and 5 hours (n=3)	Airflow rate = 85 liters/min RH = 8 ± 2%
Relative humidity	10 ± 2, 30 ± 2 and 70 ± 2% (n=4)	Loading time = 0 Airflow rate = 85 liters/min
Mono-dispersed aerosol test (MAT) ***(Particle size from 20 to 200 nm)***		
None	None	Loading time = 0 Airflow rate = 85 liters/min RH = 8 ± 2%

CHAPTER 3

RESULTS AND DISCUSSION

3.1. PHASE 1: Particle penetration against poly-dispersed NaCl aerosols in the range 15 to 200 nm at constant airflow condition (PAT method)

3.1.1. Initial particle penetration as a function of inhalation flow rate

The N95 respirators were challenged with poly-dispersed NaCl aerosols for a period of 5 minutes at each of four constant flow rates: 85, 135, 270 and 360 liters/min using the experimental set-up described above (see Figure 2-2 on p.15). Figure 3-1 shows the initial particle penetration values at four constant flow rates when challenged with 15 to 200 nm poly-dispersed sodium chloride aerosols. The test was repeated three times at each flow rate with a new respirator. The peak and standard deviation of initial penetration values were computed at each particle diameter with respect to the flow rate.

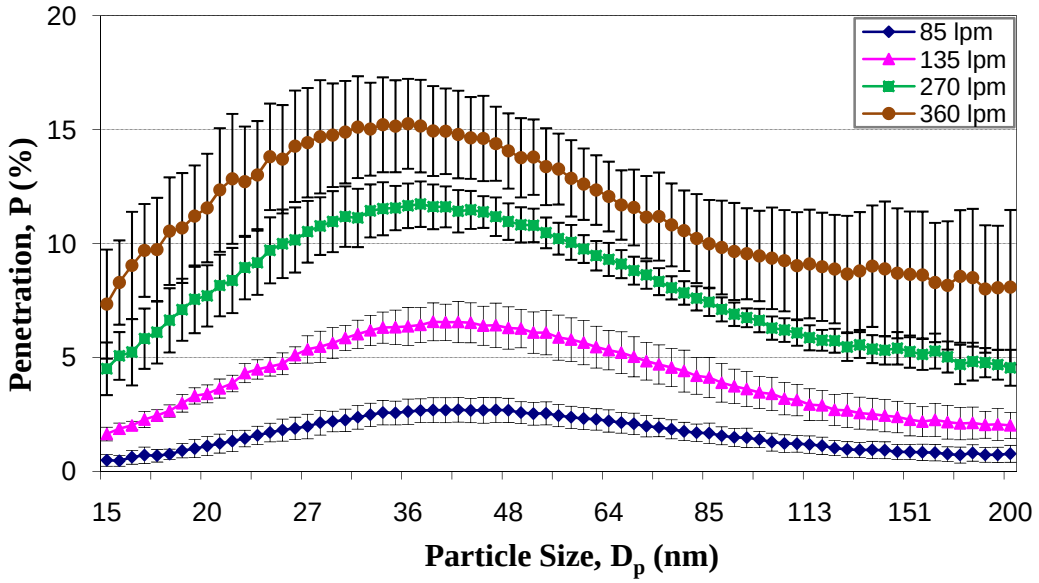

Figure 3-1: Effect of particle size and inhalation flow rate on initial particle penetration through N95 respirators (n=3). The error bars represent the standard deviations.

Consistent with the results from previous studies, the initial particle penetration was significantly increased as the flow rate increased (Balazy et al. 2006a, 2006b; Richardson et al. 2006; Huang et al. 2007; Kim et al. 2007; Eninger et al. 2008). The maximum initial penetration level through N95 respirators dramatically exceeded 5% NIOSH certification criterion at about 1.30, 2.35 and 3.05 times at high flow rates of 135, 270 and 360 liters/min, resepectively. At the MPPS, with

the lowest filtration efficiency, the percentage penetrations were 2.7 ± 0.54, 6.6 ± 0.90, 11.7 ± 1.00 and 15.3 ± 1.97% at 85, 135, 270 and 360 liters/min, repectively (Table 3-1).

Table 3-1: Summary of particle penetration, pressure drop and MPPS for PAT (mean ± std)

Airflow rate (Q) (liters/min)	Pressure drop (mm H_2O)	Maximum P (%)	MPPS (nm)
85	7.79 ± 0.27	2.7 ± 0.54	46
135	13.32 ± 1.03	6.6 ± 0.90	41
270	23.79 ± 0.77	11.7 ± 1.00	37
360	32.7 ± 0.91	15.3 ± 1.97	36

The mean initial particle penetration at 360 liters/min exceeded that at 85 liters/min by about 6-fold. In addition, according to the obtained results, with the increasing flow rate, the MPPS demonstrated a shift toward smaller particles; approximately 46, 41, 37 and 36 nm at 85, 135, 270 and 360 liters/min, respectively, results which are consistent with results from earlier studies (Martin and Moyer, 2000; Balazy et al. 2006a, 2006b; Richardson et al. 2006; Huang et al. 2007; Rengasamy et al. 2008a; Rengasamy and Shaffer, 2008b). The shift in the MPPS toward small sizes and the increase in the particle penetration are both due to the fact that, along with the increase in flow rate, the diffusion and electrostatic mechanisms contribute less to the removal of smaller particles as a result of less residence time (Richardson et al. 2006).

Furthermore, along with the increasing flow rate, the quality factor value was reduced (Figure 3-2). These dramatic drops in the quality factor values, particularly at higher flow rates, are largely attributed to the increasing pressure drop and particle penetration, which is in agreement with the literature (Han, 2000; Eninger et al. 2008).

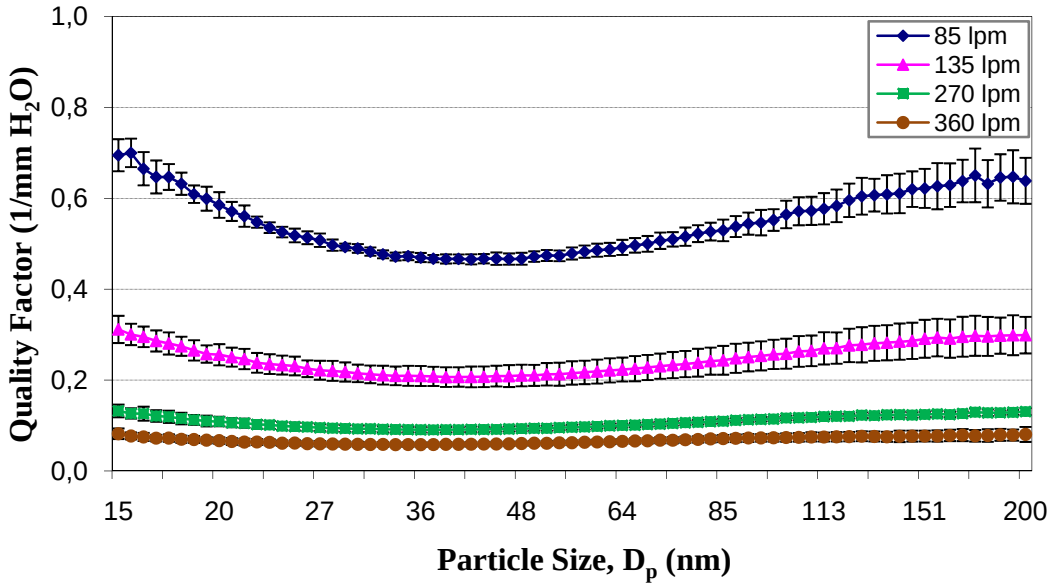

Figure 3-2: Effect of particle size and inhalation flow rate on filter quality factor of N95 respirators (n=3). The error bars represent the standard deviations.

3.1.2. Particle penetration as a function of loading time

The selected N95 respirator was loaded continuously against 15 to 200 nm poly-dispersed NaCl particles at a flow rate of 85 liters/min for a period of 5 hours. Figure 3-3 illustrates the effect of loading time on the particle penetration level through the N95 respirator. The test was repeated three times, each time with a new respirator. The peak particle penetrations and also the quality factor for the N95 respirator were determined over time (once at each hour).

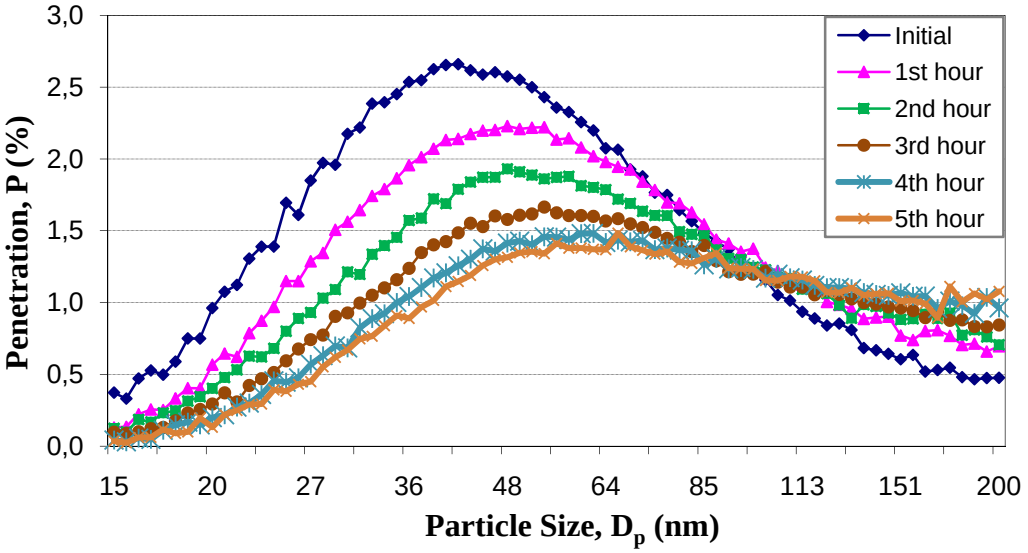

Figure 3-3: Effect of loading time on particle penetration through N95 respirators at a constant flow rate of 85 liters/min (n=3).

The results also show that for particles below 100 nm in size, penetration decreased with the loading time, while penetration increased for particles larger than 100 nm. As summarized in Table 3-2, for particles below 100 nm, the maximum penetration levels were reduced from 2.66 ± 0.21 to 1.48 ± 0.12%.

Table 3-2: Summary of particle penetration, pressure drop and MPPS in the early (A) and late (B) stage of particle loading performance (5 hours)

Airflow rate (liters/min)	Particle loading stage -------	Pressure drop (mm H_2O)	Maximum P (< 100 nm)	MPPS (nm)
85	A	7.95 ± 0.57	2.66 ± 0.21	41
85	B	10.86 ± 1.27	1.48 ± 0.12	66

As observed in Figure 3-3, the MPPS shifted toward larger particle sizes, from 41 to 66 nm for the tested N95 respirator. This is due to the fact that diffusion becomes more dominant for the collection of NPs while the electrostatic attraction force shows less contribution in capturing large size particles (Martin and Moyer, 2000, Wang, 2001; Woon et al. 2008). Moreover, less variability as a function of particle diameter in particle penetration was identified with longer particle loading time.

As mentioned earlier, the penetration for the particles between 15 to 100 nm showed a considerable reduction with the loading process, whereas, the penetration gradually increased for the larger particle sizes. Seemingly, this phenomenon could be due to the formation of particle aggregates on the surface of the filter (Wang, 2001; Woon et al. 2008). For small particles, along with the reduction in the electrostatic attraction force, greater loading time generally leads to an increase in capturing the particles by diffusion, as the deposited particles are similar in size to the approaching particles (Wang, 2001). On the contrary, the captured particles may suppress the collection of particles caused by the electrostatic attraction force, which is a noticeable collection mechanism for the large size particles predominantly between 150 to 500 nm (Wang, 2001). Experimental studies on electret filters demonstrated that the particle collection efficiency relies generally on the amount of electrostatic charge on the filter fiber (Brown et al. 1988; Chen et al. 1993; Martin and Moyer, 2000).

Figure 3-4 displays the filter quality pattern of the N95 respirator at each particle diameter during the filter loading. The results showed further discrepancy in the quality factors at larger particle sizes (the quality factor values were similar for particles between 15-30 nm for all aerosol loading times).

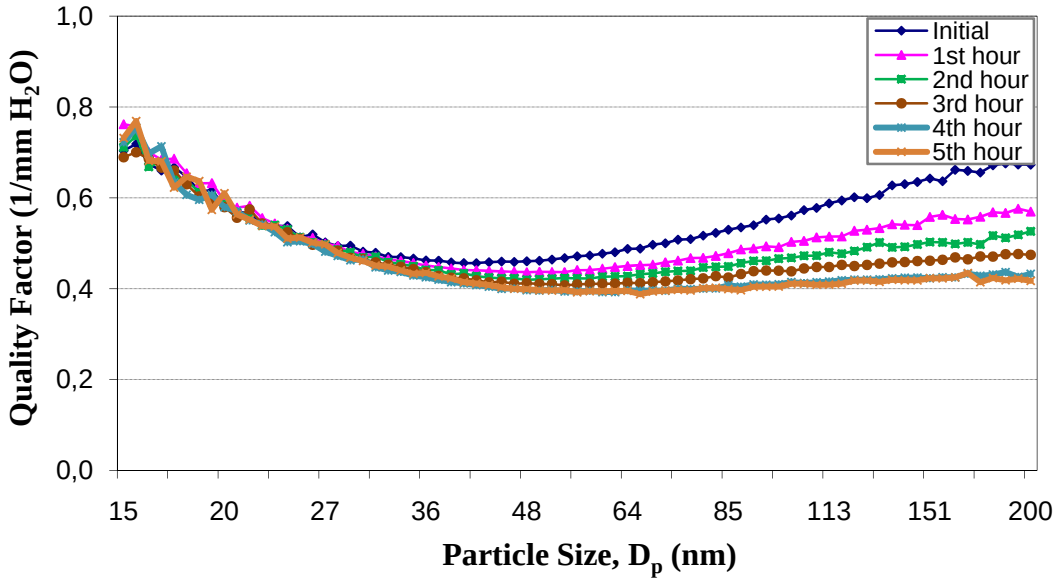

Figure 3-4: Effect of particle size and loading time on filter quality factor of N95 respirator at a constant flow rate of 85 liters/min (n=3).

3.1.3. *Particle penetration as a function of relative humidity*

The respirator was tested against 15 to 200 nm poly-dispersed NaCl particles at a flow rate of 85 liters/min at three levels of relative humidity; 10, 30 and 70% for 5 minutes. A Humidity Control System (MNR, Model HCS-301, Miller Nelson Research Inc.) was utilized to condition the relative humidity before the total air entered the inlet chamber. Figure 3-5 presents the initial penetration of sodium chloride particles through the N95 respirator at three different levels of relative humidity. Each test was repeated four times for the particles ranging from 15 to 200 nm using a new respirator. The peak and standard deviation of initial penetration levels were determined. Consistent with the results obtained from the previous studies on electret filters, for particles below 100 nm, the filtration performance decreases slightly with the increase of RH, and this is attributed to the reduction in the charges on the fiber filters and particles (Ackley, 1982; Moyer et al. 1989). However, for the large particle sizes, the penetrations were similar at 10 and 30% RH; whereas subsequently increased as RH elevated to 70%.

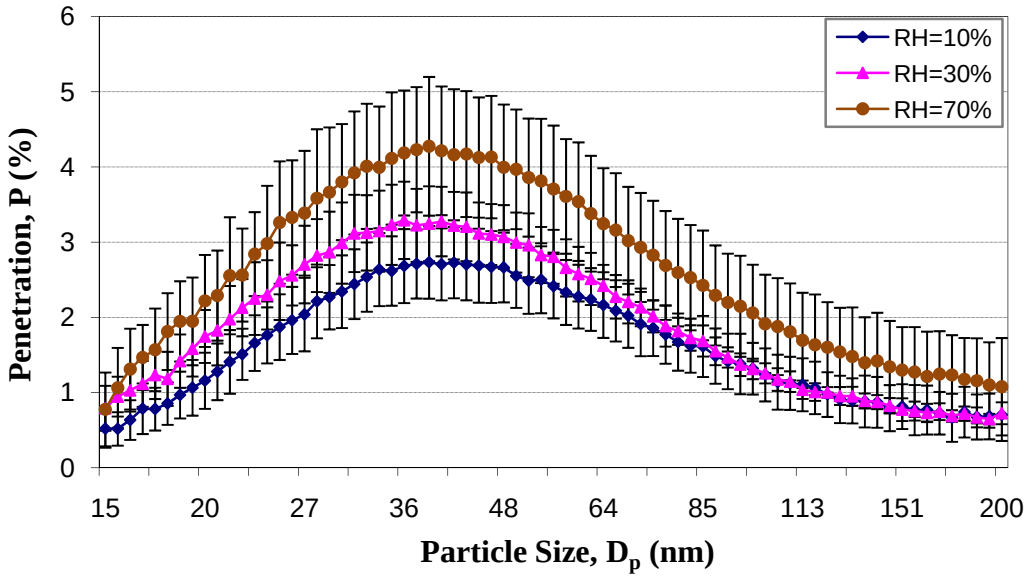

Figure 3-5: Effect of relative humidity on initial particle penetration through N95 respirators at a constant flow rate of 85 liters/min (n=4). The error bars represent the standard deviation at each point.

Even if the maximum initial penetration increased slightly with the RH, it did not exceed the 5% NIOSH certification criterion. The penetrations at the MPPS were respectively 2.73 ± 0.47, 3.30 ± 0.50 and 4.27 ± 0.90% at 10, 30 and 70% RH.

With an increase in RH, at the MPPS, no consistent shift was identified. However, the MPPS still occurred in the range between 30 to 50 nm, acknowledging the presence of electrostatic attraction mechanism on the filter particle collection. Table 3-3 provides information on the maximum penetrations and MPPS of the particle penetration (Mostofi et al. 2011).

Table 3-3: Summary of particle performance at an airflow rate of 85 liters/min

RH (%)	Maximum P (%)	MPPS (nm)
10	2.73 ± 0.47	41
30	3.30 ± 0.50	36
70	4.27 ± 0.90	39

3.2. PHASE 2: Particle penetration against mono-dispersed NaCl aerosols in the range 20 to 200 nm at constant airflow condition (MAT method)

3.2.1. Correlation of mono-dispersed and poly-dispersed particle penetration

The filtration performance of the N95 respirator was investigated against twelve different mono-sized NaCl particles (20, 30, 40, 45, 50, 55, 60, 80, 100, 120, 160 and 200 nm) at 85 liters/min constant flow rate.

Figure 3-6 illustrates the particle penetrations through N95 respirators at constant flow rate of 85 liters/min against mono-dispersed sodium chloride particles using the mono-dispersed aerosol test (MAT) method. The figure also shows the results of the measured penetrations at constant flow rate of 85 liters/min when challenged with poly-dispersed aerosols. The tests were repeated four times with each mono-sized NaCl aerosol using a new respirator. Consistent with results from previous studies with electret filters, the MPPS occurred in the 40 to 100 nm range. Higher initial penetration level was found at each tested particle size with the MAT method (Figure 3-6). However, in all cases, the initial penetration never exceeded the 5% NIOSH certification criterion at 85 liters/min. The results also revealed no relation between the initial particle penetrations, measured with MAT and PAT methods at each corresponding particle size, at 85 liters/min.

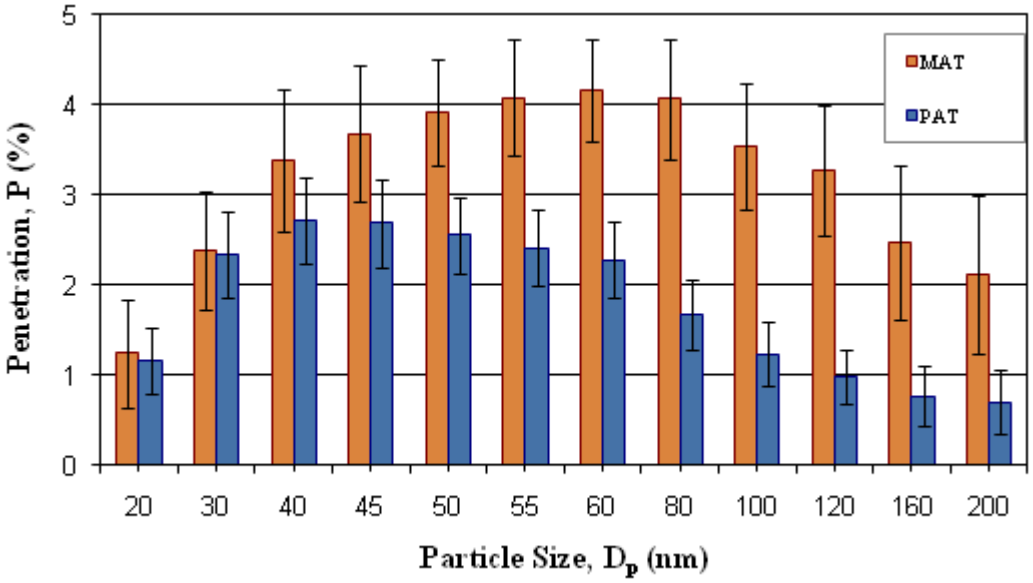

Figure 3-6: The comparison of mono-dispersed and poly-dispersed particle penetration levels (n=4). The error bars represent the standard deviation at each point.

In addition, as observed in Figure 3-7, the results showed very low number concentration of nanoparticles at the upstream of the N95 respirator compared with the measured number concentration with the PAT method, at each corresponding particle size at 85 liters/min (see Figure 2-11 on p. 21). Depending on the particle size, the number concentrations were approximately between 80 and 1600 particles/cm^3 as opposed to around 10^6 particles/cm^3 when measured with the PAT method. This low number concentration of nanoparticles is mainly due to the diffusion losses through the measuring instrument; SMPS, mainly from five parts: impactor inlet, neutralizer, tubing to the DMA and CPC, and DMA and CPC (Mostofi et al. 2012).

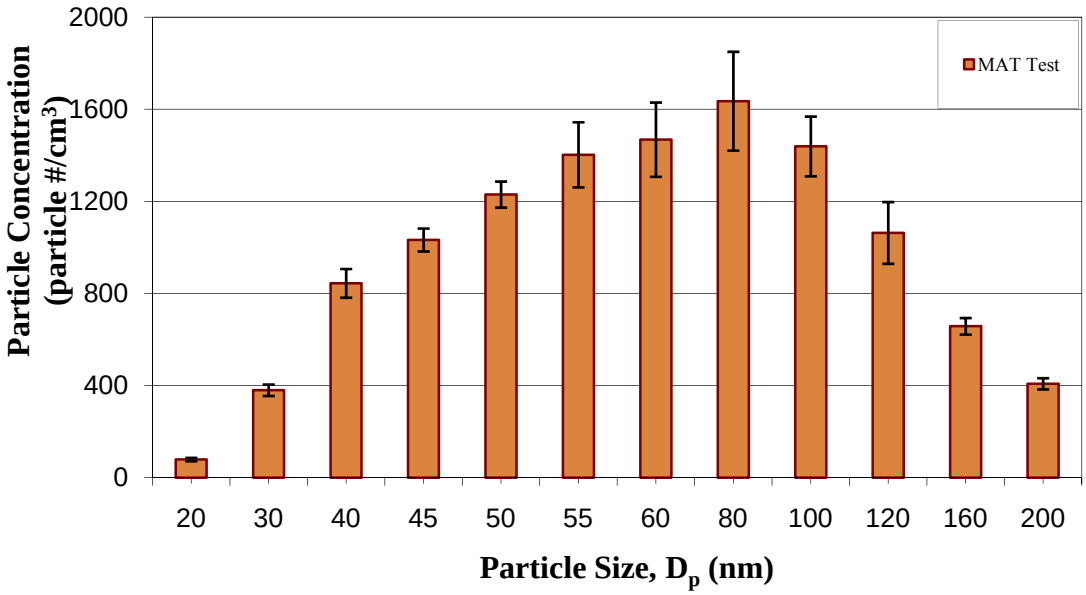

Figure 3-7: The particle number concentration at each tested mono-sized particles (n=4). The error bars represent the standard deviation at each point.

CHAPTER 4

CONCLUSIONS AND FUTURE WORKS

4.1. Conclusions and summary

A review of previous research work on the filtration performance of filters and respirators against nanoparticles was presented. It was concluded that the methodologies and protocols adopted are not standardized: the experiments are carried out at various conditions (temperature, airflow rate, RH, measurement techniques, etc.). This has limited the validation of the procedure and has made it difficult to compare results across these various studies. With the growth observed in the manufacturing sector of nano-products, it is important to study the impact of the above mentioned parameters on filter effectiveness under conditions normally found in the working environment. This is especially important given that one of the most challenging issues currently facing occupational health and safety is the lack of knowledge about the effect of airflow rate, humidity, and the duration of use on the performance of filter media for capturing nanoparticles.

Previous studies were limited to bench-top tests under high contaminant concentration and at relatively low airflow rates. Due to the conditions aforementioned, the results of these studies cannot be inferred for real applications. The majority of previous investigations demonstrated that the filter respirators were efficient for capturing particles at constant flow rates ranging between 30 and 85 liters/min. Although a flow rate of 85 liters/min simulates the relatively high breathing rate at strenuous work load used by NIOSH for respirator certification, it is believed that the inhalation rate can exceed 350 liters/min at a heavy work load.

The results of the poly-dispersed aerosol test (PAT) from the present study demonstrated that the filtration efficiency of a NIOSH approved filtering face-piece N95 respirator dropped with the increase in flow rate; the maximum initial particle penetration dramatically exceeded the 5% certification criterion at about 1.30, 2.35 and 3.05 folds, at flow rates of 135, 270 and 360 liters/min, respectively. The MPPS slightly shifted toward small particle sizes with the increase of flow rate, from 46 nm at 85 liters/min to 36 nm at 360 liters/min. The particle penetration through the N95 filtering face-piece respirator was found to decrease with further loading time for nano-sized particles, while it increased slightly for larger size particles. This phenomenon was attributed to the deposition of particles on the filter fibers surface which cloggs the pores of the filter and consequently enhances the collection of smaller particles caused by diffusion. The experimental results also showed that the performance of N95 respirators decreased slightly with the increase of RH level likely due to a reduction in electrostatic charge on the filter fibers at higher RH.

The mono-dispersed aerosol test (MAT) method was performed at 85 liters/min constant flow rate; the initial particle penetration at the MPPS was below 5% NIOSH certification criterion.

Moreover, the initial particle penetration value, measured with MAT method was higher than the one measured with PAT method at each corresponding particle size.

All the results and analyses can be summarized as follows:

1. Compared with the poly-dispersed aerosol test (PAT) method, the mono-dispersed aerosol test (MAT) method gave higher initial penetration at an airflow rate of 85 liters/min. However, in neither case, penetration exceeded 5%.
2. Increasing the airflow rate decreased the efficiency of the N95 respirators in a way that the respirator may lose its threshold efficiency of 95%. Indeed, at flow rates of 135, 270 and 360 liters/min, penetration exceeded the threshold penetration of 5%.
3. Increasing the airflow rate decreased the quality factor. This was due to a larger pressure drop and greater penetration which occured under high airflow rates.
4. At a constant flow rate, increasing the relative humidity decreased the efficiency of the N95 respirators, specifically for smaller particle sizes.
5. The efficiency of the N95 respirators increased when the respirator was challenged with NPs for longer loading times.

4.2. Future works and recommendations

The recommendations for future research work on filtration performance assessments are given below.

The developed methodology has the ability to investigate the collection efficiency of a series of filtering face-piece respirators. Thus, it is recommended to test three classes of N, R and P respirators with three levels of filter efficiency; 95, 99 and 99.97%. For each class of filters, tests should be conducted against solid and liquid particles. The poly-dispersed aerosol test (PAT) method was the predominant method used for particle generation in this research. However, more reliable research is needed to investigate the effect of mono-dispersed generation with a method which is capable of providing a considerable amount of NPs in order to show effective performances of N95 or any other types of N, P, or R-series respirators.

The method should be applicable to investigate the performance of respiratory mask filters under a realistic airflow pattern (cyclic airflow). Most previous studies were limited to test filters at constant airflow rates. However, the results of these studies cannot be inferred for real applications because, in reality, the airflow rate through a respiratory mask filter is not constant and varies according to the breathing rate. It is suggested that the performance of a filter under a periodic airflow rate would be different than that measured under a constant airflow rate.

Last but not least, improved guidance in the selection and use of respirators against NPs should be developed to ensure a high level of respiratory protection for workers and exposed persons.

REFERENCES

Ackley, M.W. (1982). *Degradation of Electrostatic Filters at Elevated Temperature and Humidity.* 3rd World Filtration Congress, pp. 169–176.

Alonso, M., Kousaka, Y., Hashimoto, T. & Hashimoto, N. (1997). *Penetration of Nanometer-Sized Aerosol Particles through Wire Screen and Laminar Flow Tube.* Journal of Aerosol Science, 27, 471–480.

ASHRAE. Standard 52.2. (2007). *Method of Testing General Ventilation Air-Cleaning Devices for Removal Efficiency by Particle Size.* American Society of Heating, Refrigerating, and Air-Conditioning Engineers, Inc., Atlanta.

Balazy, A., Podgorski, A. & Gradon, L. (2004). *Filtration of Nano-sized Aerosol Particles in Fibrous Filters. I- Experimental Results*. Journal of Aerosol Science, 35, 967–968.

Balazy, A., Toivola, M., Adhikari, A., Sivasubramani, S.K., Reponen, T. & Grinshpun, S.A. (2006a). *Do N95 Respirators Provide 95% Protection Level against Airborne Viruses, and How Adequate Are Surgical Masks?* American Journal of Infection Control, 34, 51–57.

Balazy, A., Toivola M., Repoen T., Podgorski A., Zimmer A., & Grinshpun S.A. (2006b). *Manikin-Based Performance Evaluation of N95 Filtering Face-Piece Respirators Challenged with Nano-particles.* Annals of Occupational Hygiene, 50, 259–269.

Baumgartner, H., Loffler, F. & Umhauer, H. (1986). *Deep-Bed Electret Filters-The Determination of Single Fbre Charge and Collection Efficiency.* IEEE Transactions on Electrical Insulation, 21, 477–486.

BGI. (2002). *Collision Nebulizer-Instructions. MRE 1, 3, 6 and 24 Jet.* BGI Incorporated.

Boskovic, L., Agranovski, I.E. & Braddock, R.D. (2007). *Filtration of Nanosized Particles with Different Shape on Oil Coated Fibres.* Journal of Aerosol Science, 38, 1220-1229.

Boskovic, L., Agranovskia, I.E., Altmana, I.S. & Braddocka, R.D. (2008). *Filter Efficiency as a Function of Nano-Particle Velocity and Shape.* Journal of Aerosol Science, 39, 635–644.

Brown, R.C., Wake, D., Gray, R., Blackford, D.B. & Bostock, G.J. (1988). *Effect of industrial aerosols on the performance of electrically charged filter material.* Annuals of Occupational Hygiene, 32(3): 271-294.

Brown, R.C. (1993). *Air Filtration: An Integrated Approach to the Theory and Applications of Fibrous Filters.* Oxford U.K.: Pergamon.

Chen, C.C., Lehtimäki, M. & Willeke, K. (1993). *Loading and filtration characteristics of filtering facepieces.* American Industrial Hygiene Association Journal, 54(2), 51–60e.

Chen, C.C. & Huang, S.H. (1998). *The Effect of Particle Charge on the Performance of a Filtering Face-Piece.* American Industrial Hygiene Association Journal, 59, 227–233.

Code of Federal Regulations (CFR). (1996). *Approval of Respiratory Protective Devices.* Title 42, Part 84, pp. 528–593.

Crooks, M. (2007). *Nano-Safty and Instrumentation.* NanoMicroClub Networking Event. Presented by Crooks (TSI Inc.), 22nd May in Oxford.

Davies, C.N. (1973). *Air Filtration.* Academic Press, London.

De la Mora, J. F., De Juan, L., Eichler, T. & Rosell, J. (1998). *Differential Mobility Analysis of Molecular Ions and nanometer Particles.* TrAC Trends in Analytical Chemistry, 17, 328–339.

Department of Health and Human Services (DHHS). (2003). *Guidance for Filtration Air Cleaning System to Protect Building Environments from Airborne Chemical, Biological, and Radiological Attacks.* Publication 2003–136.

Donaldson, K., Stone, V., Clouter, A., Renwick, L. & MacNee, W. (2001). *Ultrafine Particles.* Journal of Occupational and Environmental Medicine, 58, 211–216.

Dockery, D.W. & Pope, A.C. (1994). *Acute Respiratory Effects of Particulate Air Pollution.* Annual Review of Public Health, 15, 107–132.

Dullien, F.A.L. (1989*). Introduction to Industrial Gas Cleaning,* Academic Press, San Diego.

Eninger, R.M., Honda, T., Adhikari, A., Tanski, H., Reponen, T. & Grinshpun, S.A. (2008). *Filter Performance of N99 and N95 Face-Piece Respirators against Viruses and Ultrafine Particles.* Annals of Occupational Hygiene, 52, 385–396.

Fjeld, R. & Owens, T. (1988). *The Effect of Particle Charge on Penetration in an Electret Filter.* IEEE Transactions on Industry Applications, 24, 725–731.

Grafe, T., Gogins, M., Barris, M., Schaefer, J. & Canepa, R. (2001). *Nanofibers in Filtration Applications in Transportation.* Proceedings of the Filtration 2001 International Conference and Exposition of the INDA (Association of the Nowovens Fabric Industry), Chicago, IL; 1-15.

Han, D.H. (2000). *Performance of Respirator Filters Using Quality Factor in Korea*. Industrial Health Journal, 38, 380–384.

Hagdnagy, W., Stiller-Winkler, R., Kainka, R., Ranft, U. & Idel, H. (1998). *Influence of Urban Air Pollution on the Immune System of Children.* Journal of Aerosol Science, Supplement 2, S997–S998.

Hinds, W.C. (1999). *Aerosol Technology: Properties, Behavior, and Measurement of Airborne Particles.* (2nd ed.), NewYork: Wiley.

Howard, J. (2003). *Guidance for filtration an air-cleaning systems to protect building environments from airborne chemical, biological, or radiological attacks.* http://www.cdc.gov/niosh/docs/2003-136/pdfs/2003-136.pdf. Accessed February 15, 2009.

Huang, S.H., Chen, C.W., Chang, C.P., Lai, C. Y. & Chen, C.C. (2007). *Penetration of 4.5 nm to 10 µm Aerosol Particles through Fibrous Filters.* Journal of Aerosol Science, 38, 719–727.

Ikezaki, K., Iritani, K., Nakamura, T. & Hori, T. (1995). *Effect of Charging State of Particles on Electrets.* Journal of Electrostatics, 35, 41–46.

Janssen, L. (2003). *Principles of Physiology and Respirator Performance.* Occupational Health & Safety, 72, 73–81.

Ji, J.H., Bae, G.N., Kang, S.H. & Hwang, J. (2003). *Effect of Particle Loading on the Collection Performance of an Electret Cabin Air Filter for Submicron Aerosols.* Journal of Aerosol Science, 34, 1493–1504.

Kanaoka, C., Emi, H., Otani, Y. & Liyama, T. (1987). *Effect of Charging State of Particles on Electret Filtration.* Journal of Aerosol Science, 7, 1–13.

Kim, C.S., Bao, L., Okuyama, K., Shimada, M. & Niinuma, H. (2006). Filtration Efficiency *of a Fibrous Filter for Nano-Particles.* Journal of Nanoparticle Research, 8, 215–221.

Kim, S., Harrington, M. & Pui, D. (2007). *Experimental Study of Nano-Particles Penetration through Commercial Filter Media*. Journal of Nanoparticle Research, 9, 117–125.

Kousaka, Y., Okuyama, K., Shimada, M. & Takii, Y. (1990). *Development of a Method for Testing Very High-Efficiency Membrane Filters for Ultrafine Aerosol Particles.* Journal of Chemical Engineering of Japan, 23, 568–574.

Lee, K.W. & Liu, B. (1980). *On the Minimum Efficiency and the Most Penetrating Particle Size for Fibrous Filters.* Journal of the Air Pollution Control Association, 30, 377–381.

Lowkis, B., & Motyl, E. (2001). *Electret Properties of Polypropylene Fabrics.* Journal of Electrostatics, 51-52, 232–238.

Martin, S.B. & Moyer, E.S. (2000). *Electrostatic respirator filter media: filter efficiency and most penetrating particle size effects.* Applied occupational and Environmental Hygiene, 15, 609–617.

Miguel, A.F. (2003). *Effect of Air Humidity on the Evolution of Permeability and Performance of a Fibrous Filter during Loading with Hygroscopic and Non-Hygroscopic Particles.* Journal of Aerosol Science, 34, 783–799.

Mostofi, R., Noël, A., Haghighat, F., Bahloul, A., Lara, J. & Cloutier, Y. (2012). *Impact of Sampling Measuring Techniques on the Performance of N95 Respirator against Ultrafine Particles*, Int. Journal of Hazardous Materials, 217-218:51-57.

Mostofi, R., Bahloul, A. Lara, J., Wang, B., Cloutier, Y. and Haghighat, F. (2011). *Investigating of Potential Affecting Factors on Performance of N95 Respirator*, J. of the International Society for Respiratory Protection, 28: 26-39

Mostofi, R., Wang, B., Haghighat, F., Bahloul, A. & Lara, J. (2010*) Performance of Mechanical Filters and Respirators for Capturing Nanoparticles – Limitations and Future Directio*, Int. J. Industrial Hygiene, 48: 296-304.

Moyer, E.S. & Stevens, G.A. (1989). *''Worst Case'' Aerosol Testing Parameters: II. Efficiency Dependence of Commercial Respirator Filters on Humidity Pre-treatment.* American Industrial Hygiene Association Journal, 50, 265–270.

National Institute for Occupational Safety and Health (NIOSH) and the Bureau of Labor Statistics (BLS). (2003). *Respirator Usage in Private Sector Firms.* Department of Health and Human Services & Department of Labor.

Nemmar, A., Vanbilloen, H., Hoylaerts, M., Hoet, P., Verbruggen, A. & Nemery, B. (2001). *Passage of Intratracheally Instilled Ultrafine Particles from the Lung into the Systemic Circulation in Hamster.* American Journal of Respiratory and Critical Care Medicine, 164, 1665–1668.

Nemmar, A., Hoet, P., Vanquickenborne, B., Dinsdale, D., Thomeer, M., Hoylaerts, MF., Vanbilloen, H., Mortelmans, L. & Nemery, B. (2002). *Passage of Inhaled Particles into the Blood Circulation in Humans.* Circulation, 105, 411–414.

Oberdorster, G. (2000). *Toxicology of Ultrafine Particles: in Vivo Studies.* Philosophical Transactions of the Royal Society A, 358, 2719–2740.

Oberdorster, G., Sharp, Z., Atudorei, V., Elder, A., Gelein, R., Lunts, A., Kreyling, W. & Cox, C. (2002). *Extrapulmonary Translocation of Ultrafine Carbon Particles Following*

Whole-Body Inhalation Exposure of Rats. Journal of Toxicology and Environmental Health, Part A, 65, 1531–1543.

Oberdorster, G., Sharp, Z., Atudorei, V., Elder, A., Gelein, R., Kreyling, W. & Cox, C. (2004). *Translocation of Inhaled Ultrafine Particles to the Brain.* Inhalation Toxicology, 16, 437–445.

Oberdorster, G. (2005). *Nanotoxicology: An Emerging Discipline Evolving from Studies of Ultrafine Particles.* Environmental Health Perspectives, 113, 823–839.

Ostiguy, C., Soucy, B., Lapointe, G., Woods, C. & Ménard, L. (2008). *Les effets sur la santé reliés aux nano-particules*, Rapport IRSST R–558, 2e édition.

Rengasamy, S., Verbofsky, R., King, W.P., Eimer, B.C. & Shaffer, R.E. (2007). *Nano-Particle Penetration through NIOSH-Approved N95 Filtering Face-Piece Respirators.* Journal of the International Society for Respiratory Protection, 24, 49–59.

Rengasamy, S., King, W.P., Eimer, B.C. & Shaffer, R.E. (2008a). *Filtration Performance of NIOSH-Approved N95 and P100 Filtering Face-Piece Respirators against 4 to 30 Nanometer-Size Nano-Particles.* Journal of Occupational and Environmental Hygiene, 5, 556–564.

Rengasamy, S., Eimer, B.C. & Shaffer, R.E. (2008b). *Nano-Particle Filtration Performance of Commercially Available Dust Masks.* Journal of the International Society for Respiratory Protection, 25, 27–41.

Richardson, A.W., Eshbaugh, J.P. Hofacre, K.C. & Gardner, P.D. (2006). *Respirator Filter Efficiency against Particulate and Biological Aerosols under Moderate to High Flow Rates.* U.S. Army Edgewood Chemical Biological Center Report for Contract No. SP0700-00-D-3180. http://www.cdc.gov/niosh/npptl/researchprojects/pdfs/CR-085Gardner.pdf.

SCENIHR. (2006). *The Appropriateness of Existing Methodologies to Assess the Potential Risks Associated with Engineered and Adventitious Products of Nanotechnologies.* Directorate C–Public Health and Risk Assessment. C7–Risk Assessment. Scientific Committee on Emerging and Newly Identified Health Risk.

Takenaka, S., Karg, D., Roth, C., Schulz, H., Ziesenis, A., Heinzmann, U., Chramel, P. & Heyder, J. (2001). *Pulmonary and Systemic Distribution of Inhaled Ultrafine Silver Particles in Rats.* Environmental Health Perspectives, 109, 547–551.

Tran, C.L., Buchanan, D. & Cullen, R.T. (2000). *Inhalation of Poorly Soluble Particles. II. Influence of Particle Surface Area on Inflammation and Clearance.* Inhalation Toxicology, 12, 1113–1126.

TSI. (2003). *Model 3012A Aerosol Neutralizer Instructions.* TSI Incorporated.

TSI. (2005). *Model 3936 Scanning Mobility Particle Sizer Spectrometer Instructions.* TSI Incorporated.

Wang, C.S. (2001). *Electrostatic Forces in Fibrous Filters- A Review.* Powder Technology, 118, 166–170.

Warheit, D.B., Webb, T.R., Colvin, V.L., Reed, K.L. & Sayes, C.M. (2007a). *Pulmonary Bioassay Studies with Nanoscale and Fine-Quartz Particles in Rats: Toxicity Is Not Dependent Upon Particle Size But on Surface Characteristics.* Toxicological Sciences, 95, 270–280.

Warheit, D.B., Webb, T.R., Reed, K.L., Frerichs, S. & Sayes, C.M. (2007b). *Pulmonary Toxicity Study in Rats with Three Forms of Ultrafine-TiO2 Particles: Differential Responses Related to Surface Properties.* Toxicological Sciences, 230, 90–104.

Wiedensohler, A. (1998). *An Approximation of the Bipolar Charge Distribution for Particles in the Submicron Size Range.* Journal of Aerosol Science, 19, 387–389.

Woon, W., Leung, F. & Hunga, C.H. (2008). *Investigation on Pressure Drop Evolution of Fibrous Fiter Operating in Aerodynamic Slip Regime under Continuous Loading of Sub-Micron Aerosols.* Separation and Purification Technology, 63, 691–700.

Yang, S. & Lee, G.W.M. (2005). *Filtration Characteristics of a Fibrous Filter Pretreated with Anionic Surfactants for Mono-dispersed Solid Aerosols.* Journal of Aerosol Science, 36, 419–437.

APPENDIX A: SYSTEM CALIBRATION

Prior to the filtration efficiency test, in order to provide reliable operating conditions for the test rig and sampling procedures, some calibration and qualification tests are conducted. These calibration tests involve:

- Conducting "no filter test" (correlation test) to quantify the accuracy of the fractional efficiency measurement;
- Measuring the size distribution at different locations at upstream, to assure the dispersal uniformity of the challenge aerosol in the test chamber;
- Measuring the concentration and size distribution of the challenge aerosol using different NaCl solution concentrations; and
- Conducting the stabilization test during the system start-up to determine the time interval until the particle concentration reaches a steady condition at upstream.

"No filter test" calibration

The purpose of this test is to quantify the accuracy of the fractional efficiency measurement. The experiment similar to the filtration efficiency tests was conducted without any removal device.

To evaluate the mentioned criterion, the correlation ratio (R) was computed between two sampling locations at the upstream (center) and downstream, with all four airflow rates: 85, 135, 270 and 360 liters/min (Figures A-1 through A-4). This correlation ratio (R) is defined as:

$$R = \frac{Downstream\ Particle\ Number\ Concentration}{Upstream\ Particle\ Number\ Concentration}$$

The data analysis yielded a fairly normal deviation between the upstream and downstream concentration in both constant and cyclic phases, satisfying the last updated requirements in the ASHRAE testing standard 52.2 (2007). At the constant flow condition, the maximum and minimum values of R were 1.1 and 0.92, respectively.

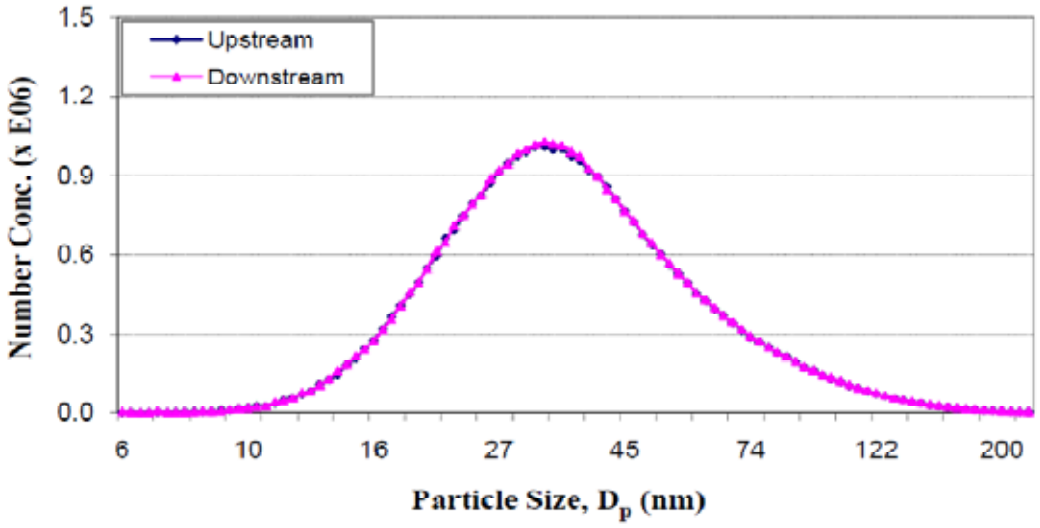

Figure A-1: Penetration without the test filter at an airflow rate of 85 liters/min.

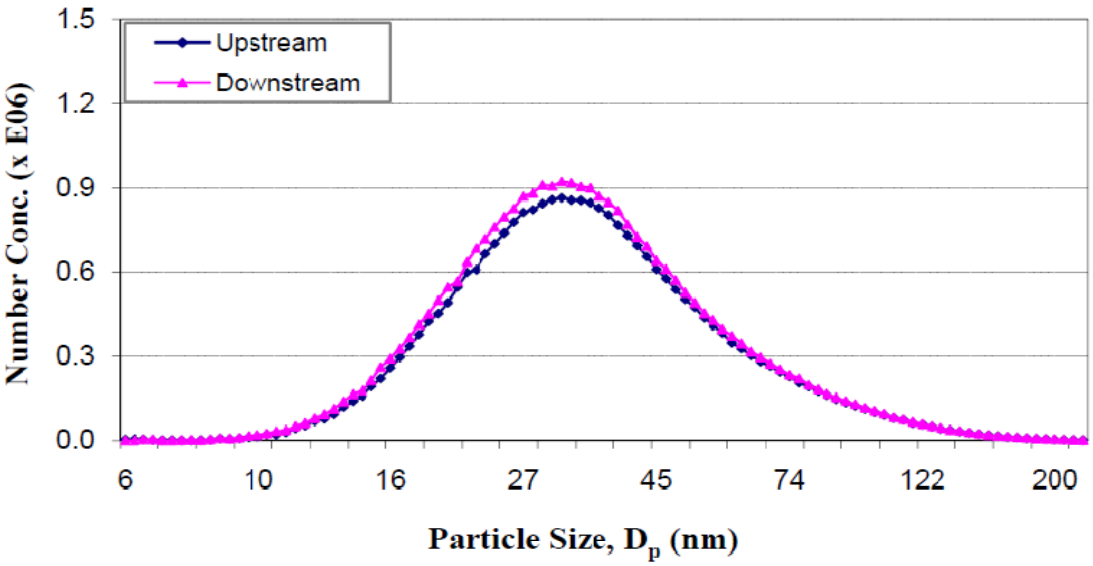

Figure A-2: Penetration without the test filter at an airflow rate of 135 liters/min.

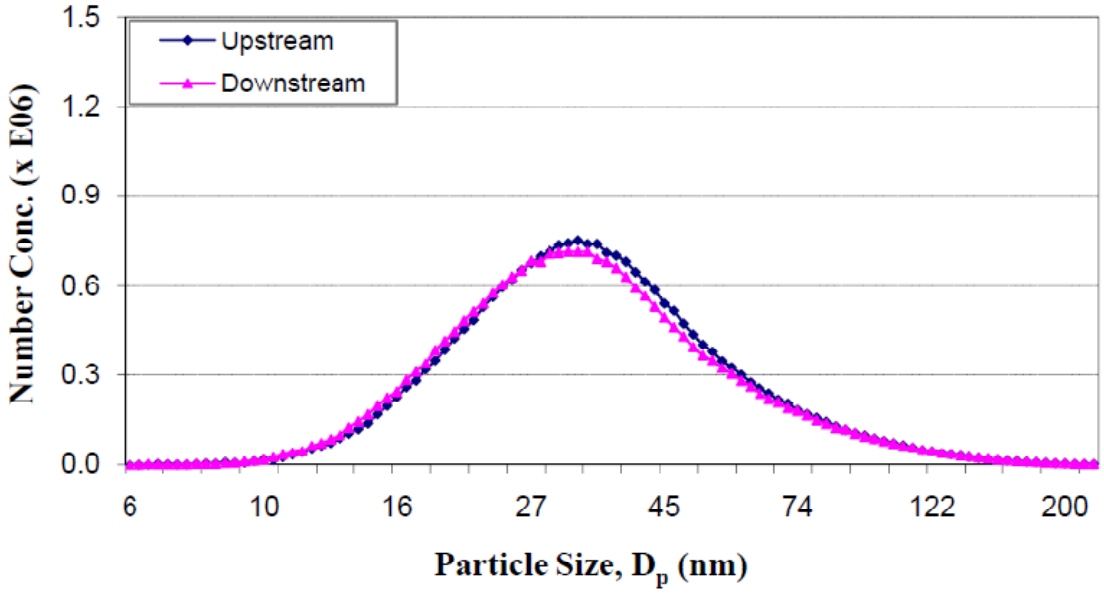

Figure A-3: Penetration without the test filter at an airflow rate of 270 liters/min.

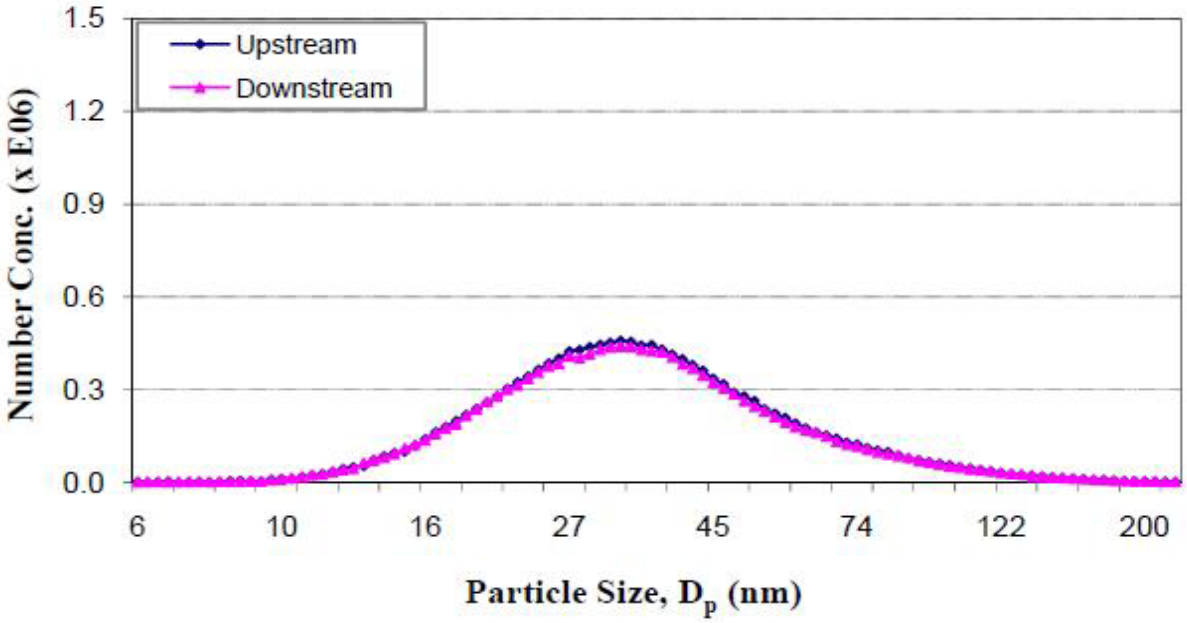

Figure A-4: Penetration without the test filter at an airflow rate of 360 liters/min.

Particle dispersal uniformity test at upstream

To verify particle dispersal uniformity, the coefficient of variation (CV) of the aerosol uniformity was calculated at five upstream sampling locations (right up, right down, left up, left down and center, Figure A-5). According to ASHRAE, the coefficient of variation must satisfy the requirements specified in the ASHRAE testing standard 52.2 (2007) (CV < 15% for each testing airflow rate) and indicated good mixing and uniformity in the test chamber.

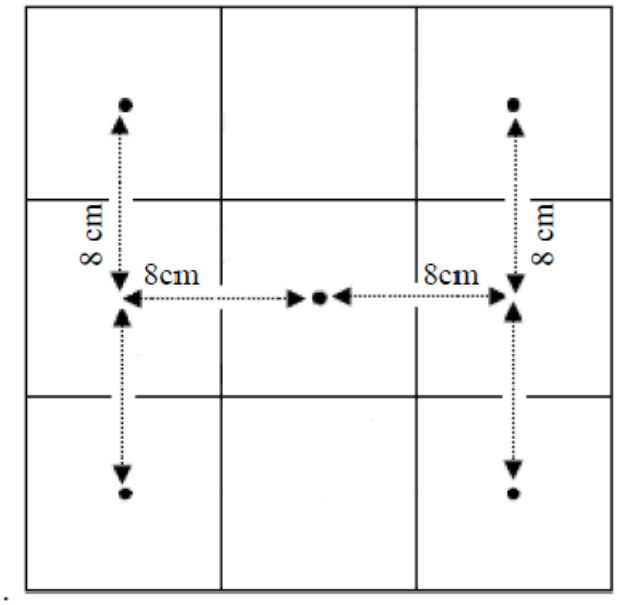

Figure A-5: Sampling positions for uniformity test.

According to the data analysis for particle sizes ranging from 6 to 200 nm, the average CV values were 4.3, 4.8, 2.8 and 5.2% at 85, 135, 270 and 360 liters/min airflow rates, respectively (Figures A-6 through A-9). In addition, Table A-1 summarizes the coefficients of variation observed for the minimum, maximum and average values.

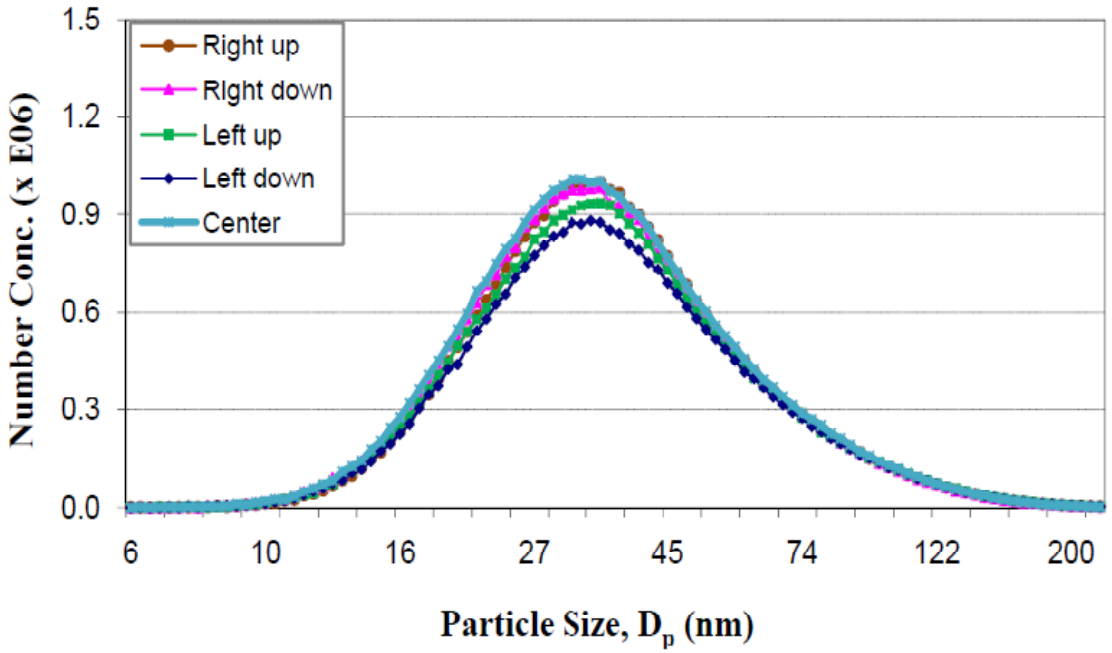

Figure A-6: Particle size distribution at five different upstream sampling locations under an airflow rate of 85 liters/min.

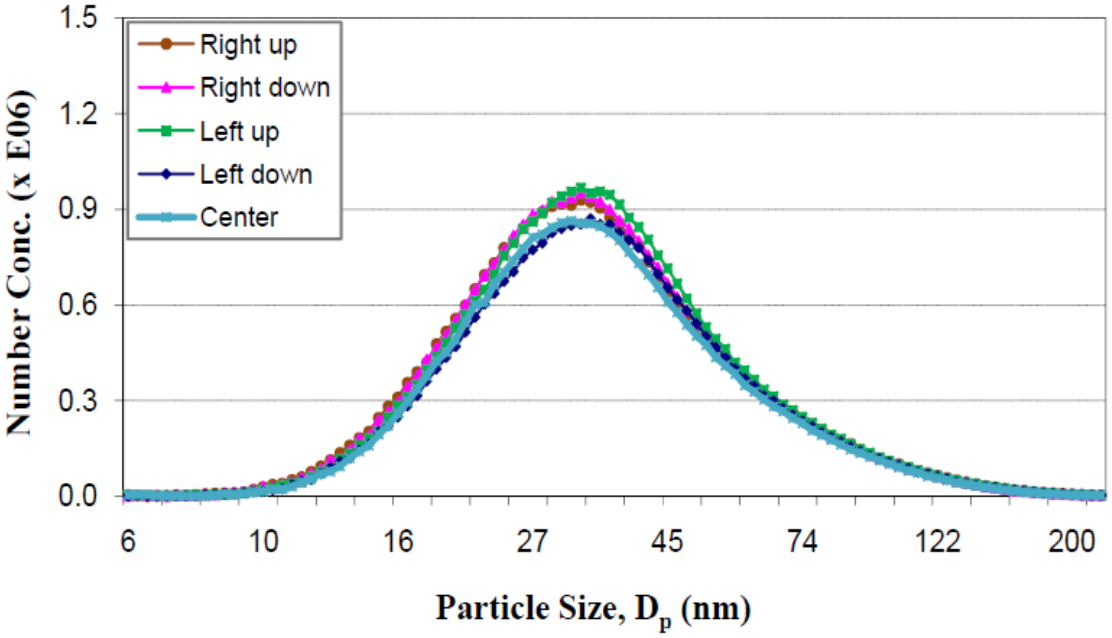

Figure A-7: Particle size distribution at five different upstream sampling locations under an airflow rate of 135 liters/min.

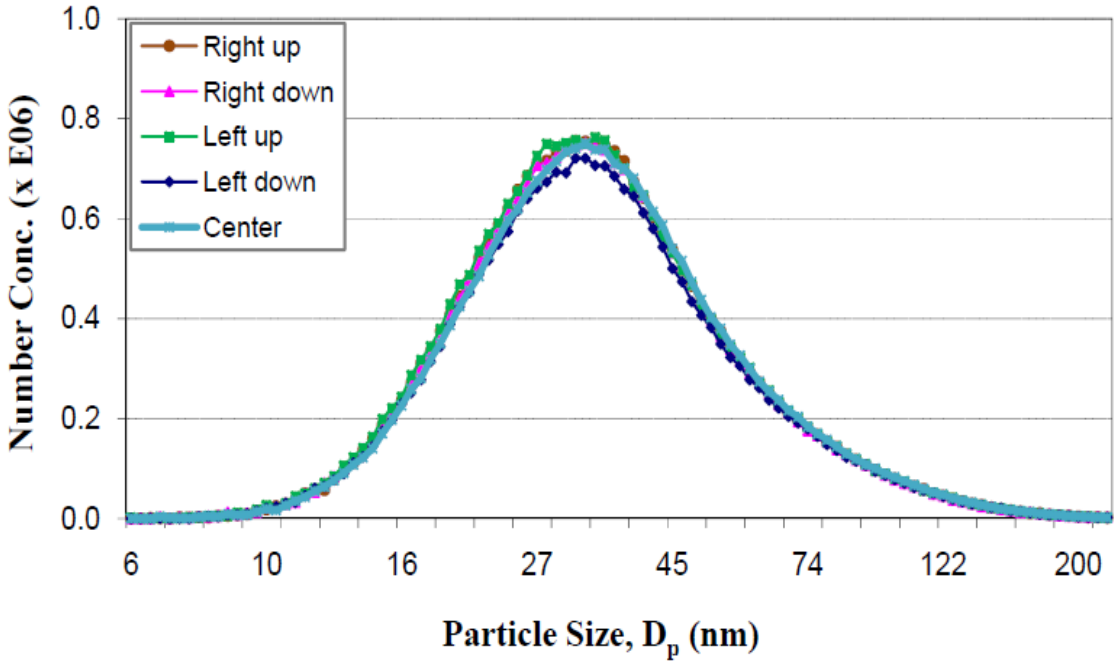

Figure A-8: Particle size distribution at five different e upstream sampling locations under an airflow rate of 270 liters/min.

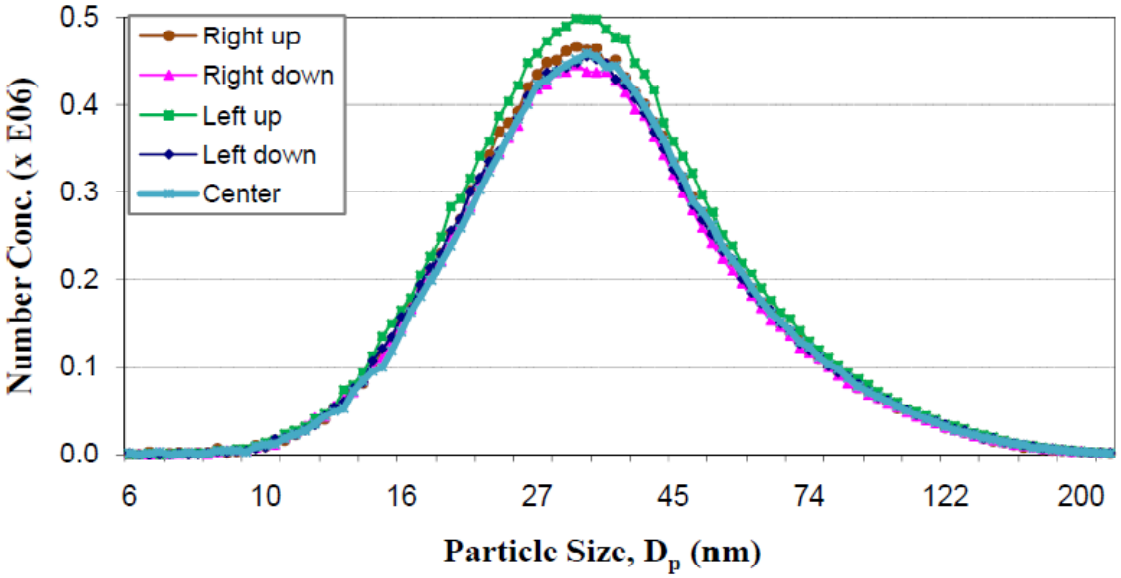

Figure A-9: Particle size distribution at five different upstream sampling locations under and airflow rate of 360 liters/min.

Table A-1: Summary of the coefficients of variation for the aerosol uniformity test

Airflow rate (liters/min)	Coefficient of variation (%)		
	Minimum	Maximum	Average
85	1.9	7.9	4.3
135	2.7	9.8	4.8
270	0.6	5.5	2.8
360	3.3	8.8	5.2

Particle size distribution at upstream

Particle concentration and size distribution were measured at the upstream of the chamber under different airflow rates of 85, 135, 270 and 360 liters/min. The six-Jet Collision Nebulizer was used to provide particles with a size ranging between 6 and 200 nm (operated at 15, 25, 30 and 35 psi inlet pressures, using 0.01, 0.1 and 1% NaCl solution concentrations, Figures A-10 through A-12). Like the previous qualification tests, the experiment was conducted without a respirator on the manikin. According to the obtained results, at the same inlet pressure, with an increase in salt solution concentration (used to generate poly-dispersed particles), the particle number concentration was found to increase at each particle diameter. The particle size distribution also demonstrated a shift toward larger sizes as the NaCl solution concentration increases.

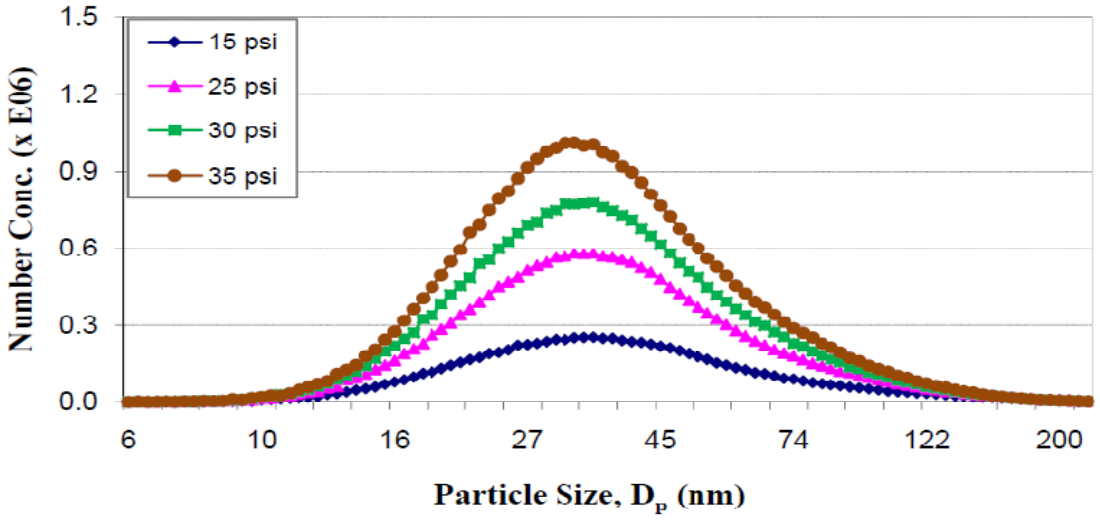

Figure A-10: Particle concentration as a function of particle size for different inlet pressures (85 liters/min and 0.01% NaCl solution).

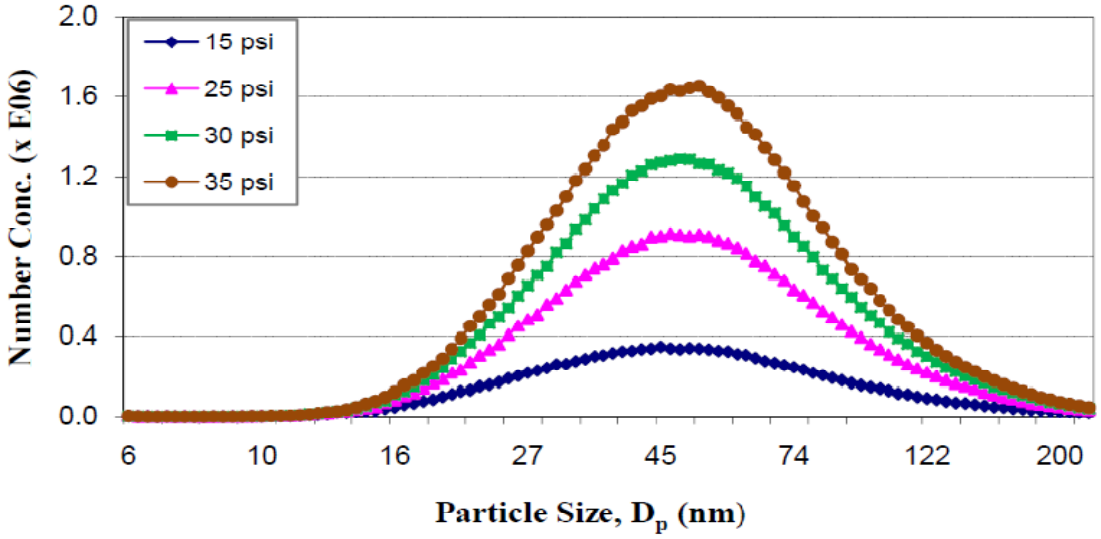

Figure A-11: Particle concentration as a function of particle size for different inlet pressures (85 liters/min and 0.1% NaCl solution).

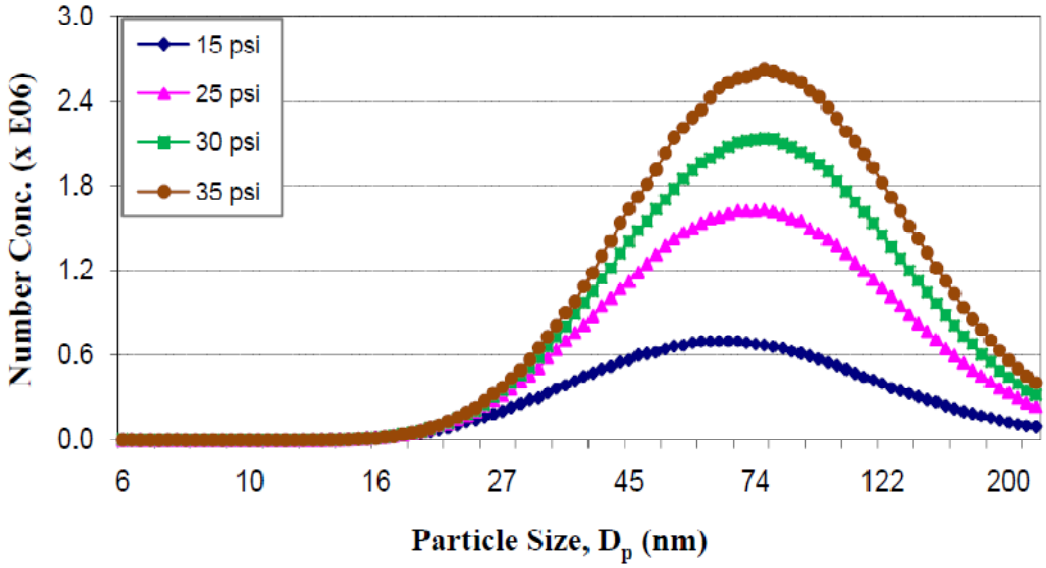

Figure A-12: Particle concentration as a function of particle size for different inlet pressures (85 liters/min and 1% NaCl solution).

Stabilization test

A stabilization test was conducted at four different constant airflow rates (85, 135, 270 and 360 liters/min) to determine the time interval required for the particles to reach a steady state concentration. The six-Jet Collision Nebulizer was operated at 35 psi inlet pressure to generate poly-dispersed NaCl particles, using a 0.01% NaCl solution.

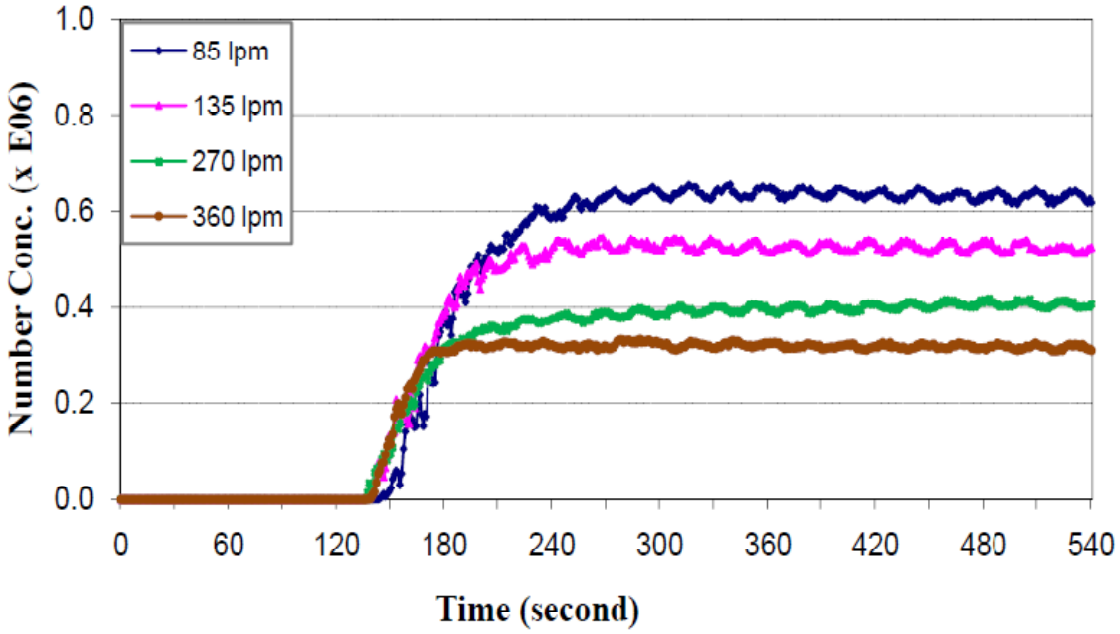

Figure A-13: Challenged aerosol concentration (particles/cm^3) during system startup for different airflow rates, using 0.01% NaCl.

In addition, as noticed in Figure A-13, small fluctuations occurred in the particle number concentration even after the stabilization period. These fluctuations occurred in a cycle nearly every 20 seconds. No explanation has been found for this phenomenon. Table A-2 presents the summarized results for the stabilization test for all four testing airflow rates.

Table A-2: Summary of results of the stabilization test

Airflow (liters/min)	Stabilization time (min)	Particle concentration (x E06 particles/cm^3)
85	1.95	0.63 ± 0.01
135	1.35	0.54 ± 0.01
270	0.82	0.40 ± 0.02
360	0.57	0.32 ± 0.06

APPENDIX B: NANOPARTICLE MEASURING INSTRUMENTS

Various measurement techniques have been developed to determine the characteristics of NPs. These methods include: mass concentration, number concentration and size distribution. As mentioned earlier, the scanning mobility particle sizer (SMPS) has been employed in this study to measure particle concentration and size distribution based on the particle electrical mobility (inversely proportional to the particle diameter). This advanced technique is capable of measuring particles ranging from 4 to 10000 nm. The SMPS mainly consists of a particle size classifier (Electrostatic classifier with a differential mobility analyzer (DMA)) and a particle detector (condensation particle counter, (CPC)). The particle size classifier classifies the charged particles based on their electrical mobility (or electrical mobility diameter). Particles with a narrow range of electrical mobility are able to exit from the DMA and then are counted by the CPC.

Particle size classifier

Figure B-1 shows the schematic diagram of the electrostatic classifier with a long DMA (model 3081, TSI Inc.). In this system, the aerosol flow is first passed through a radioactive bipolar charger in the electrostatic classifier before entering the DMA, in order to provide a bipolar equilibrium charge on the aerosols. Then, the particles are selected in the DMA according to their electrical mobility.

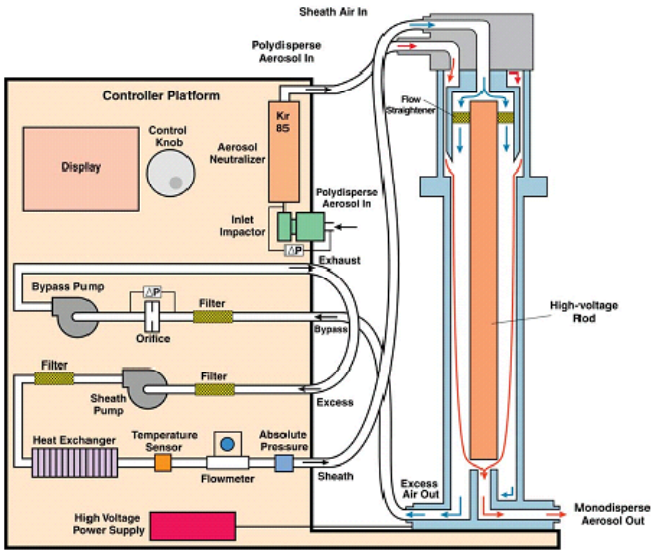

Figure B-1: Schematic diagram of the Electrostatic classifier with a long DMA, model 3081. Adapted from TSI Inc., 2005.

As shown in Figure B-1, the DMA contains an outer, grounded cylinder and an inner cylindrical electrode which is connected to a negative power supply (0 to 10 kV - DC). The electric field

between the two concentric cylinders separates the particles according to their electrical mobility (which is inversely related to the particle size). Particles with negative charges are deposited on the outer wall, whereas those with positive charges move rapidly towards the negatively-charged center electrode. Only size selected particles within a narrow range of electrical mobility have the correct trajectory to exit the DMA. The electrical mobility of these selected particles is affected by various parameters including the flow rate, the geometric parameters and the voltage of the center electrode. The size selected particles exiting from the DMA are then counted by the CPC.

Particle size distributions are measured by changing the voltage between the inner and outer cylindrical electrodes in the DMA, which changes the electric field. The DMA voltage (V) is related to the electrical mobility, Z, and to the mobility diameter, d, by the following equation:

$$Z = \frac{Qln(\frac{R_2}{R_1})}{2\pi LV} = \frac{0.441(\frac{k_B T}{M})^{0.5}}{pd^2}$$

where R_1 and R_2 are the inner and outer radii of the DMA, L is the DMA length from the inlet to the outlet slit, Q is the carrier gas flow rate, k is the Boltzmann constant, and T, p, and M are respectively the temperature, pressure and molecular weight of the carrier gas (De la Mora et al. 1998). For more specific information, review the TSI manual for series 3080 electrostatic classifiers.

Condensation particle counter (CPC)

The condensation particle counter is normally used as a part of a SMPS to count the number of particles greater than a few nanometers in diameter. Particle detection and counting is provided by a simple optical detector after a supersaturated vapor of 1-butanol condenses on the particles, causing them to grow larger. Figure B-2 presents a schematic diagram of a CPC and its various components, in a closer view.

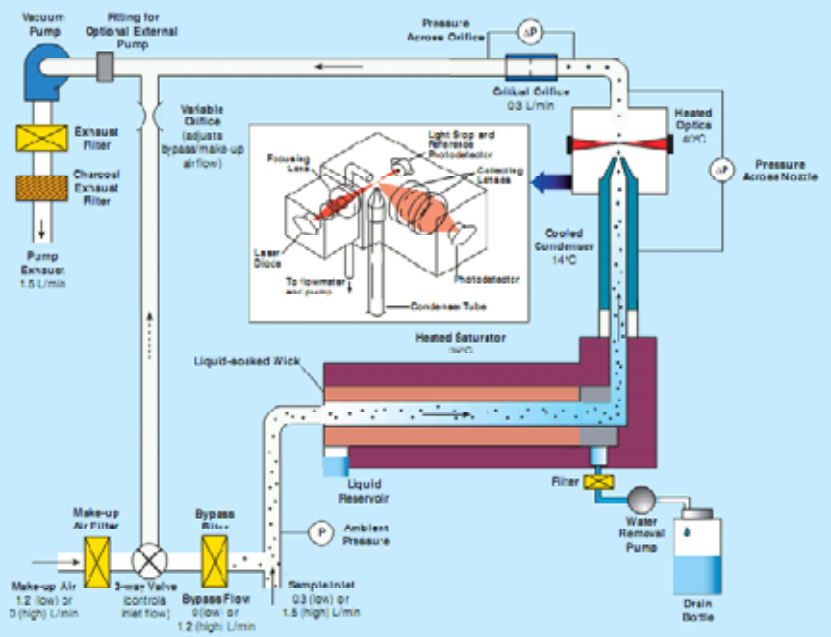

Figure B-2: Schematic diagram of a condensation particle counter, model 3775. Adapted from TSI Inc., 2005.

In the CPC, single particles larger than 2 nm are grown to micrometer size by means of condensation of a fluid (alcohol or water) on the particles. The CPC then optically counts these particles. For more detailed information, review the TSI manual for the CPC, model 3775.

APPENDIX C: PARTICLE NEUTRALIZER

The particles are required to be charge-neutralized before entering the test chamber. This is especially vital when the generated particles carry a considerable amount of charge. To minimize this problem, a neutralizer instrument (3012A Model, TSI Inc.) is used to either eliminate or reduce the possible positive and negative charges carried by the particles (Figure C-1). As the particles enter the neutralizer, they become exposed to positive and negative air ions. These air ions are attracted to oppositely charged particles causing the level of possible charge on the particles to reduce significantly.

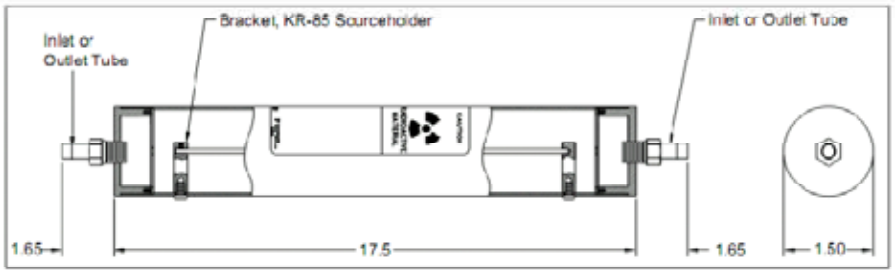

Figure C-1: Model 3012A Aerosol Neutralizer. Adapted from TSI Inc., 2003.

By providing sufficient residence time, Boltzmann charge equilibrium will be obtained for the particles. The following table displays an approximation of the charge distribution for the particles in nano-sized range, carried out by Wiedensohler, (1998) (Table C-1). In spite of particle neutralization, a portion of particles still carry a charge which becomes greater at larger particle size. Note that the 3012A model aerosol neutralizer uses a radioactive source (10 milligrams of Kr-85) to provide negative and positive air ions.

Table C-1: Distribution of charges on aerosol according to Gunn Formules (Wiedensohler, 1998)

	Percent of Particle Carrying N_p Elementary Charge Units												
$D_p(\mu m)$	-6	-5	-4	-3	-2	-1	0	+1	+2	+3	+4	+5	+6
0.01						5.14	90.75	4.11					
0.02					0.02	10.96	80.57	8.64	0.01				
0.04					0.54	19.50	64.79	14.86	0.31				
0.06				0.02	1.92	24.32	54.13	18.51	1.09	0.01			
0.08				0.11	3.72	26.81	46.73	20.46	2.10	0.05			
0.10				0.37	5.63	27.31	42.28	20.91	3.30	0.17			
0.20		0.05	0.53	3.40	12.38	25.49	29.66	19.51	7.26	1.53	0.18	0.01	
0.40	0.27	1.14	3.60	8.54	15.24	20.46	20.65	15.66	8.93	3.83	1.24	0.03	0.05
0.60	1.21	3.00	6.19	10.53	14.82	17.25	16.60	13.20	8.69	4.73	2.13	0.79	0.24
0.80	2.42	4.64	7.71	11.12	13.90	15.06	14.15	11.53	8.15	4.99	2.65	1.22	0.49
1.00	3.56	5.84	8.53	11.13	12.96	13.45	12.46	10.30	7.59	5.00	2.93	1.54	0.92